Implementation of Noord-Holland Grid in RTDS

A. G. Ejigu
(Student number: 1385909)

M.Sc. Thesis Electrical Power Engineering
July 2009

DELFT UNIVERSITY OF TECHNOLOGY

FACULTY OF ELECTRICAL ENGINEERING, MATHEMATICS AND COMPUTER SCIENCE

The work for this thesis has been carried out at High-Voltage Components and Power Systems group from November 2008 to July 2009

Thesis Committee:

Prof. ir. L. van der Sluis
Dr. M. Gibescu (Supervisor)
Ir. J. F. Baalbergen (Supervisor)
Dr. ir. H. Polinder
Dr. ir. J. van Casteren

Acknowledgment

First of all I would like to say thank you to my supervisors Dr. Madeleine Gibescu and Ir. Freek Baalbergen. They helped me unreservedly throughout the past nine months. They gave me valuable comments and personal advice to achieve my goal. Without the support and encouragement of them I would not be where I'm now. It is also my pleasure to thank my thesis committee members.

I would also like to thank the members of the DEVS project for the discussion I had with you, especially Mr. Jan Bozelie for your cooperation and help to do the DIgSILENT simulations.

I would like to thank Prof. ir. L. van der Sluis and Dr. ir. G. C. Paap for their interesting class lectures that let me know more about the subject of power system and finally that helped me to join HCPS group for specialization.

I would also like to thank all professors, lecturers and other staff members of Electrical Power Engineering department for the nice time I had during the past two years.

Last not least, special thanks to my friends T. W. Shire and Y. T. Gebrekiros for the great time we had together which makes my study life joyful.

Abstract

There are different power system simulation tools on the market. Real-time digital simulator (RTDS) is one of these tools. The HCPS group of Delft University of Technology has this digital simulator. RTDS simulator has a detailed component model library called RSCAD and a dedicated hardware for computation. The hardware is based on digital signal processors (DSP) stacked into a rack. Each rack has 21 DSPs that are capable to simulate 54 three phase nodes[1]. RTDS simulator has also the advantage to exchange signals with external device. Hence, it is used to test protective and control equipment.

In this master thesis the Noord-Holland 150 kV and 380 kV grid is implemented in RTDS. Due to the size of the grid and number of components, it was necessary to divide the whole Noord-Holland grid between different racks. For data exchange during simulation, parts of the grid model in each rack must be interconnected to each other using travelling wave transmission lines. These travelling wave transmission lines must have a travel time at least equal to an integration time step used that is equal to a single computational time (a minimum time required to solve the equations of a component model).

According to the lines LC parameters, not all lines have a travel time that is greater than or equal to the integration time step used. To have the required travel time the LC parameters of these interconnecting lines must be increased, i.e. the length of the lines has to be increased. This results in increased line impedance and different line flows in the grid. In RTDS there is also another simulation option, non-real time simulation. In non-real time simulation it is possible to decrease the integration time step required for a given computation time. So in non-real time simulation the integration time step used is decreased to satisfy the minimum travel time needed for the original parameter data.

For the validation of the model the non-real time simulation results are used. The validation is done by making a load flow value comparison with the VISION model of Noord-Holland grid and the DIgSILENT model of Noord-Holland grid is used for dynamic behaviour comparison.

From the load flow comparison per unit node voltages and phase angles at each substation are more or less similar. The node voltage maximum error is within $\pm 1\%$ and the error for the phase angles is within 10%. For line current most lines also show good results with average error of less than 5%.

The dynamic behaviour comparison is done based on short-circuit simulations at different substations. The response from both RTDS and DIgSILENT models gave nearly the same results for the voltage-dips during short-circuit fault. However, the post-fault behaviours are not exactly the same but they are comparable. After clearing

[1] A node is any junction point between power system components. For single line diagram the maximum nodes are 54/3=**18**, i.e. it is possible to implement a network that has only 18 nodes in a single rack.

the short-circuit fault the RTDS model gives more stable response than the DIgSILENT model, i.e. in the RTDS model the oscillations damp faster.

The existing Noord-Holland grid is expanded into a future scenario with a large wind power plant. The wind power plant is implemented using a constant PQ source model with a low voltage ride through algorithm. According to previous work this model is used to represent a HVDC connected off-shore wind power plant. This simplified model is enough for grid stability study of large systems. Based on this model 1200 MW active power with a given coupling point power factor is injected at the Velsen 150 kV substation. The connection of the wind power plant raises the voltage level at all substations by more than 3% on average. Relatively the dynamic behaviour of the expanded grid is less stable compared to the existing grid.

List of abbreviations

List of abbreviations used for substations

VLN	Velsen
APL	Anna Paulowna
WYW	Wijdewormer
NDK	Noord Klaprozenweg
HK	Hoogte Kadijk
VW	Venserweg
BZ	Bijlmer Zuid
AMV	Amstelveen
VHZ	Vijfhuizen
HMM	Haarlemmermeer
BN	Bijlmer Noord
OTL	Oterleek
DMN150	Diemen 150 kV
GVL	s-Graveland
HW	Hemweg
NMR	Nieuwe Meer
WEW	Westwoud
DMN380	Diemen 380 kV
OSZ	Oostzaan
BVW	Beverwijk

Other abbreviations

RTDS	Real-Time Digital simulator
PSSE	Power Systems Simulation for Engineers
DIgSILENT	Digital SImuLator for Electrical NeTwork
PSAT	Power System Analysis Toolbox
SPS	SimPowerSystems
AVR	Automatic Voltage Regulator
DSP	Digital Signal Processor
HCPS	High-Voltage Components and Power Systems
HVDC	High Voltage Direct Current
DG	Distributed Generation
CHP	Combined Heat and Power
EMT	Electromagnetic Transient
RMS	Root Mean Square
SVC	Static Var Compensator
DSL	Dynamic Simulation Language
GUI	Graphical User Interface
SCIG	Squirrel Cage Induction Generator
DFIG	Double Fed Induction Generator
FCSG	Full Converter Synchronous Generator
PWM	Pulse Width Modulation
VSC	Voltage Source Converter

List of symbols

ψ_d	Stator flux linkage in the d-axis
e_d	Stator winding voltage in the d-axis
R_a	Stator winding resistance
i_d	Stator winding current in the d-axis
ψ_q	Stator flux linkage in the q-axis
e_q	Stator winding voltage in the q-axis
i_q	Stator winding current in the q-axis
L_d	Stator winding inductance in the d-axis
L_{ad}	Mutual inductance between stator and rotor windings in the d-axis
i_{fd}	Field winding current
i_{1d}	d-axis damper winding current
L_q	Stator winding inductance in the q-axis
L_{aq}	Mutual inductance between stator and rotor windings in the q-axis
i_{1q}	q-axis damper winding current
ψ_{fd}	Field winding flux linkage
e_{fd}	Field winding voltage
R_{fd}	Field winding resistance
ψ_{1d}	d-axis damper winding flux linkage
R_{1d}	d-axis damper winding resistance
ψ_{1q}	q-axis damper winding flux linkage
R_{1q}	q-axis damper winding resistance
L_{ffd}	Field winding inductance
L_{11d}	d-axis damper winding inductance
L_{11q}	q-axis damper winding inductance
T_m	Mechanical torque
T_e	Electrical torque
ω_s	Synchronous speed
ω_r	Rotor speed
δ	Load angle
H	Inertia constant
C_p	Power coefficient
λ	Tip speed ratio

Table of contents

Chapter 1

Introduction

1.1 Background

A traditional power system grid has a structure with a top-down power flow (vertical hierarchy). In most cases the large centralized power generating units, either thermal, steam or hydro, produce the electric power demanded by the consumers. Then this power is delivered to its end-users through high voltage transmission lines and distribution network. Depending on the length of these lines, there is significant transmission loss during power transmission.

Nowadays, however, the existing grid structure is changing from vertical to horizontal power flow hierarchy. The main driving factor for this change is the availability of abundant renewable energy sources at end-user location, lower and medium voltage levels. The increasingly strong environmental concern and increasing oil price are also increase the need for renewable power source.

As a result of this, the interest of generating electric power using distributed generating units is increasing. Hence, in the future power grid system more and more decentralized generation (DG) units, like wind turbines, solar panels and combined heat and power (CHP) units that use renewable energy sources will be present. Most of these sources inject the power at lower and medium voltage levels hence they change the power flow trend. Since they are close to the end-user location, transmission power loss will be minimized.

These DG units have an influence on the technical aspects of the power grid; of course the severity depends on the penetration level of decentralized generation. As large wind farms are connecting to the grid, the grid operators need to know the way how it affects the grid behaviour. In the future there will be a huge amount of offshore wind power. So, this is the right time to figure out and deal with the possible technical influence of these sources on the grid stability.

This Master thesis is part of DEVS (Dynamic State Estimation and Voltage Stability) project which is a joint project of TU Delft, ECN, KEMA and Liandon. The objective of DEVS is to measure current and voltage in the future power grid in order to asses the actual stability of the system and to test control strategies before they are taken into use. The HCPS group of TU Delft has a Real-Time Digital Simulator (RTDS). In RTDS it is possible to do a real-time simulation of power grid and to interact with this grid via analogue and digital input/output ports.

Before carrying out these tests and assessments it is necessary to implement the existing grid with possible future scenario expansions in RTDS. As the first step, the Noord-Holland grid will be implemented in this Master thesis Project.

1.2 Thesis outline

The objective of this project is to implement the test grid for Noord-Holland with future scenario extensions in RTDS. The RTDS model will be implemented using the existing Noord-Holland grid model that is available in VISION and DIgSILENT. These models are used as a source material for grid parameters. Once the model implemented in RTDS, it is possible to conduct a real-time dynamic simulation of this test grid under different conditions. Further more it is also possible to use this model as a test grid in the future for possible proposed tests.

Main tasks of this thesis project are;

- Implementation of existing Noord-Holland grid (150 kV and 380 kV) in RTDS.
- Extension of the grid to future scenario with large wind power plant.
- Finally, validate the RTDS model and conduct dynamic tests.

The organization of this thesis is as follows:

Chapter-2: literature review of power system behaviour and simulation methods. The features of RTDS are also discussed.

Chapter-3: in this chapter the implementation of existing Noord-Holland in RTDS and its validation are discussed.

Chapter-4: this chapter deals with the extension of the existing grid with large wind power plant. The existing technologies of wind turbines are discussed plus how the simplified wind power plant is implemented in RTDS. Then, simulation results from the expanded grid are discussed.

Chapter-5: conclusions and recommendations are given.

Chapter 2

Review of Power System Behaviour and Simulation Methods

2.1 Power system behaviour

The behaviour of power system is related to its ability of responding to the change in energy/power balance of a system, i.e. the ability to store a fraction of energy change into its electrical and mechanical components during power unbalance. Depending on the response time for the power unbalance there are three ways in which the power system can store a fraction of the energy; primary energy conversion, mechanical inertia and passive electrical components (LC parameters of the grid). As a result of this energy storing and transferring, there are three phenomena that occur in power system [1].

Electromagnetic phenomena

Electrical transient of the network are within time scale of 10^{-6} seconds to 10^{-3} seconds. In this phenomenon the system tries to store the fraction of energy in its electrical components like the inductors and capacitors. But the charging and discharging time constants of these components are very small. Hence, the resulted transient phenomena can have large oscillation within this time frame.

Electromechanical phenomena

Dynamic response of system generators due to their rotating inertia is within time scale of 10^{-3} seconds to 10 seconds. In this phenomenon the system tries to store a fraction of the energy into its mechanical component (the rotor of the machines) in terms of its rotor angle δ. Compared to the electrical components the mechanical component has larger time constant to store the energy change.

Thermodynamic phenomena

The energy conversion process from primary energy sources within time scale of seconds to hours. In this phenomenon the large fraction of energy change can be controlled by monitoring the conversion of the primary energy source. The response time is longer compared to the other phenomena.

A major element of power system analysis is the determination of the group of energy storage or exchange transients that are appropriate to the study of each specific problem. So the complexity of power system simulation analysis and component modelling depends on the desired phenomena under investigation.

2.2 Power system simulation methods

Corresponding to the above power system phenomenon there are at least three types of simulation methods: electromagnetic transient, power system dynamic and power dispatch (load flow) simulations.

Electromagnetic Transient (EMT) simulation

It is also called instantaneous value simulation is use to simulate an electromagnetic transient phenomena. For this simulation method the model of the power system components is complex as smaller time constant parameters are considered. To solve the equations of the network model the required time step is in μs.

Power System Dynamic (RMS) simulation

This simulation method deals with electromechanical transients and neglects the electromagnetic transients of the network. Hence, it considers only the fundamental frequency components of voltage and current. The complexity of the component models is reduced by neglecting differential equations that involve smaller time constant parameters. Hence, compared to EMT simulation longer time step can be used to solve the network equation. A typical time step used for power system dynamic simulation is 10 ms.

Load flow and power dispatch simulation

This simulation method is used to solve the steady state power flow equations of the network. The time constant for the steady state operation (thermodynamic process of primary energy conversion) is in the order of several seconds to minutes. So all the differential equations involved in the network model are assumed to be constant. Hence the power flow equations become algebraic equations that can be solved using an iteration method like Newton-Raphson method.

Depending on the power system phenomena to be dealt with, the behaviour of the power system component has to be modelled with the corresponding detailed algebraic and differential equations.

2.3 Power System Representation

According to [2] overall power system representation includes models for the following individual components:

- Synchronous generators and the associated excitation system and prime movers governor system.
- Interconnecting transmission network including static loads.
- Induction and synchronous motor loads or dynamic loads.
- Other devices such as HVDC converters and SVCs

2.3.1 Synchronous generators and the associated excitation system and prime movers

The synchronous generator model is a combination of different equations: equation of motion, rotor circuit equation and stator voltage equation. It might be interesting to consider the magnetic saturation effect too. The model of the generator can be represented in different degree of complexity depending on the assumptions made and interest of power system phenomena to be dealt with.

The stator circuit equations of a synchronous generator are given in equation (2.1). All parameters are in pu.

$$\frac{\mathrm{d}}{\mathrm{dt}}\psi_d = e_d + R_a i_d - \omega_r \psi_q$$
$$\frac{\mathrm{d}}{\mathrm{dt}}\psi_q = e_q + R_a i_q + \omega_r \psi_d \qquad (2.1)$$

Where the d and q axis flux linkages are given by:

$$\psi_d = -L_d i_d + L_{ad} i_{fd} + L_{ad} i_{1d}$$
$$\psi_q = -L_q i_q + L_{aq} i_{1q}$$

Similarly the rotor circuit equations of the synchronous generator are given in equation (2.2). These equations hold for one q-axis damper winding system.

$$\frac{d}{dt}\psi_{fd} = e_{fd} - R_{fd} i_{fd}$$
$$\frac{d}{dt}\psi_{1d} = -R_{1d} i_{1d} \qquad (2.2)$$
$$\frac{d}{dt}\psi_{1q} = -R_{1q} i_{1q}$$

Where,

$$\psi_{fd} = -L_{ad} i_d + L_{ffd} i_{fd} + L_{ad} i_{1d}$$
$$\psi_{1d} = -L_{ad} i_d + L_{ad} i_{fd} + L_{11d} i_{1d}$$
$$\psi_{1q} = -L_{aq} i_q + L_{11q} i_{1q}$$

The rotor torque or motion equations are given in equation (2.3):

$$\frac{d}{dt}\omega_r = \frac{[T_\mathrm{m} - T_e]}{2\omega_s H}, \text{ where } T_e = \psi_\mathrm{d} i_\mathrm{q} - \psi_\mathrm{q} i_\mathrm{d}, \ \omega_r = \text{rotor speed (pu)}$$
$$\frac{d}{dt}\delta = \omega_r - 1 \text{ , where 1 is the rated } \omega_\mathrm{s} \text{ in pu} \qquad (2.3)$$

In the stator voltage equations, $\frac{\mathrm{d}}{\mathrm{dt}}\psi_d$ and $\frac{\mathrm{d}}{\mathrm{dt}}\psi_q$ influence the electromagnetic transients of the electric network. Terms in the rotor motion equations influence the behaviour of electromechanical transient response. The number of differential equations required depends on the interest of transient phenomenon to be dealt. For electromechanical transient simulation the terms in equation (2.1), $\frac{\mathrm{d}}{\mathrm{dt}}\psi_d$ and $\frac{\mathrm{d}}{\mathrm{dt}}\psi_q$ can be assumed constant and ω_r is also assumed equal to 1 pu. Hence, the numbers of differential equations that are involved in the stator voltage equation are decreased.

The degree of saturation in the magnetic circuit is different for the d-axis and q-axis fluxes. For example the q-axis flux path of salient pole rotor is mostly through the air gap, so it is possible to neglect the q-axis saturation effect. For stator magnetic circuits it is possible to represent the effect of saturation in different ways like by taking two saturation parameters corresponding to 1.0 and 1.2 pu terminal voltage on the open-circuit saturation curve of the machine or more accurately by taking up to ten points on the open-circuit saturation curve of the machine.

The excitation and governor control systems of the generator should also modelled appropriately. Each control system either excitation or governor can be represented with differential equation; respectively to control the excitation field voltage and the input mechanical torque. For example equation (2.4) shows a diode rectifier excitation control system.

$$\frac{d}{dt}E_{fd} = \frac{K_a(V_{ref} - V_t - V_s) - K_e E_{fd}}{t_e}$$

$$\frac{d}{dt}V_s = \frac{K_f \frac{d}{dt}E_{fd} - V_s}{t_f} \qquad (2.4)$$

An example of a typical steam turbine governor model is also described as shown in equation (2.5).

$$\frac{dT_m}{dt} = \frac{Ft_2 \frac{dx}{dt} + x - T_m}{t_2}$$

$$\frac{dx}{dt} = \frac{K(\omega_{ref} - \omega_r) - x}{t_1}, \text{ where } \frac{1}{\mathrm{K}} = R \text{ (droop)} \qquad (2.5)$$

2.3.2 Interconnecting transmission network

To model a transmission line there are two possibilities, either the lumped (it can be T or PI equivalent circuit) or distributed parameter (travelling wave) line model can be used. When the travelling time of the signal over the transmission line is less than the simulation time step, the PI equivalent circuit is appropriate. For example, for integration time step of 50 μs and propagation velocity of $3*10^8$ m/s, all transmission

lines with a length of less than 15 km are represented by the PI equivalent circuit. When the travelling time of the signal is larger then the integration time step, it is better to use the travelling wave line model.

2.3.3 Induction and synchronous motor loads

The synchronous motor can be modelled in the same way as synchronous generator. The direction of the power flow is however different. Even for the case of an induction motor it is possible to use the same procedure as that of the synchronous motor. For induction machine case the following differences have to be taken into account: the rotor has symmetrical structure, rotor speed varies with load and there is no excitation voltage source applied to the rotor windings. As a result for induction machine the dynamics of the rotor circuit is determined by the slip.

2.4 Mathematical tools to solve power system equations

The model of a given power system component is represented by a combination of algebraic and differential equations. So, mathematical tools like iterative methods and numerical integration methods are required to solve the algebraic equations and differential equations respectively.

2.4.1 Iterative methods to solve algebraic equations of power flow

To perform the time domain analysis first the initial state of the system must be determined by calculating the power flows and node voltages for specified bus conditions. At the terminal of the bus a source, a load or a transmission line can be connected. Depending on the type of the component connected to the bus, either active power, reactive power, voltage magnitude or phase angle can be specified.

Using the current injection equation and node admittance matrix of the network, the iteration algorithm can be developed to estimate the value of a state variable till the error converges to specified tolerance.

According to [2] the current injection equation and admittance matrix of the network are described by the following equations. Equation (2.6) shows the injection of current I_k at node k with node voltage V_k and power flow of P_k and Q_k. Equation (2.7) shows the current injection in relation with the node admittance matrix Y_{kk} and node voltage V_k.

$$\overline{I_k} = (P_k - jQ_k) / \overline{V_k}^* \tag{2.6}$$

$$\overline{I_k} = Y_{kk}\overline{V_k} + \sum_{i=1, i\neq k}^{n} (Y_{ki}\overline{V_i}),\ i = 1...n \tag{2.7}$$

The above two equations are the heart of the iteration algorithm. There are different iteration methods to solve the algebraic (linear and nonlinear) equation of power flow; like Gauss-Seidel and Newton Raphson methods.

Gauss-Seidel method: this technique is the oldest method used to solve a linear system of equations. For a set of linear equations expressed in matrix form the values of the variables can be calculated using this method but convergence can be granted only for symmetric or diagonal dominance matrix.

From the above equations, the iteration equation for Gauss-Seidel method can be derived as given by equation (2.8):

$$\overline{V_k} = \frac{P_k - jQ_k}{Y_{kk}\overline{V_k}^*} - \frac{1}{Y_{kk}} \sum_{i=1, i\neq k}^{n} (Y_{ki}\overline{V_i}) \tag{2.8}$$

Generally this method has the following advantages for power system linear equations.

- Simple, reliable and usually tolerant of poor voltage and reactive power conditions.
- Low computer memory requirement.
- Computational time increases with system size.

The disadvantage of this method is the slow convergence rate (because of the weak diagonal dominance of the node admittance matrix).

Newton-Raphson method: the best known method to solve non-linear algebraic equations in power system analysis. For fast convergence of this method the iteration should start with values that are nearly close to desired values (initial guess of voltage and angle must be close to the desired final value) otherwise the convergence is poor.

The iteration equation for Newton-Raphson method is derived form equations (2.6) and (2.7) as shown below.

$$P_k + jQ_k = \overline{V_k} \sum_{i=1}^{n} (Y_{ki}^* \overline{V_i}^*)$$

$$P_k = V_k \sum_{i=1}^{n} (G_{ki}V_i \cos\theta_{ki} + B_{ki}V_i \sin\theta_{ki})$$

$$Q_k = V_k \sum_{i=1}^{n} (G_{ki}V_i \sin\theta_{ki} - B_{ki}V_i \cos\theta_{ki})$$

After some mathematical simplification, the change in P_k and Q_k at each node can be defined as a function of changes in V and θ as shown in equation(2.9).

$$\begin{bmatrix}\Delta P\\ \Delta Q\end{bmatrix} = J\begin{bmatrix}\Delta\theta\\ \Delta V\end{bmatrix},\ \text{where } J = \begin{bmatrix}\frac{\partial P}{\partial\theta} & \frac{\partial P}{\partial V}\\ \frac{\partial Q}{\partial\theta} & \frac{\partial Q}{\partial V}\end{bmatrix} \text{ is the Jacobian matrix.} \quad (2.9)$$

This method has the following advantages.

- For reasonable initial guess this method has very good convergence rate, at least quadratic.
- Computational time depends on the size of problem.
- Suitable for large systems requiring very accurate solution.
- The iteration process repeated until the errors are lower than a specified tolerance.

The disadvantage of this method is that with a poor initial value guess of V and θ it will not converge.

Fast decoupled load-flow (FDLF) method

As mentioned in [2], this method neglects the weak dependence between P-V and Q-θ. As a result it neglects the terms $\frac{\partial P}{\partial V}$ and $\frac{\partial Q}{\partial\theta}$ of the Jacobian matrix. By applying these simplifications to a Jacobian matrix of Newton-Raphson method the computation of ΔP and ΔQ can be done as shown below in equation (2.10). The Jacobian matrix has an impact on the convergence of the iteration solution but does not directly affect the final solution [2].

$$\begin{aligned}\Delta P &= \frac{\partial p}{\partial\theta}\Delta\theta\\ \Delta Q &= \frac{\partial Q}{\partial V}\Delta V\end{aligned} \quad (2.10)$$

The approximation result in small increase in number of iteration but reduce the memory requirement.
The advantages of this method are:

- Reduces memory requirement.
- Its convergence rate is linear.
- Less sensitive to the initial voltage and reactive power conditions.
- Provide rapid solution with good accuracy.

2.4.2 Numerical integration methods to solve differential equations

In power system analysis there are not only algebraic equations but also differential equations. To solve a given differential equation $f(V,t)=\frac{dV}{dt}$, it is possible to apply either of the following methods.

a) Euler Method: first order numerical integration procedure, it uses the first two terms of Taylor series as shown in equation (2.11), for solving ordinary differential equations with a given initial value. This method is numerically less stable for stiff equations than other methods. Along with its slow error convergence this method is not often used for complex numerical integration.

$$V_{n+1} = V_n + \Delta V$$
$$\Delta V = \Delta t\left(\frac{dV}{dt}\Big|_{V=V_n}\right), \text{ where } V = f(V_n, t_n) \tag{2.11}$$

For sufficient accuracy the time step Δt has to be small otherwise the windup or propagation of error will result in numerical instability. However smaller time steps take more computational time and the propagation error may affect the numerical stability. To overcome this limitation the Modified Euler Method can be implemented which uses predictor and corrector steps. The corrector step can be used repeatedly until successive steps converge with the desired accuracy. The limitation of Euler predictor-corrector step method is that it is not self-starting so it needs more computer storage and requires smaller time steps.

b) Runge-Kutta (R-K) Method: this method has different family of numerical integration methods depending on orders of Taylor series approximation. The most commonly used is 4th order R-K method, given in equation (2.12), with self adjusting step size and an accumulated error in the order of Δt^5.

$$V_{n+1} = V_n + \frac{1}{6}(K1 + 2K2 + 2K3 + K4) \tag{2.12}$$

Where,

$$K1 = f(V_n, t_n)\Delta t$$
$$K2 = f\left(V_n + \frac{K1}{2}, t_n + \frac{\Delta t}{2}\right)\Delta t$$
$$K3 = f\left(V_n + \frac{K2}{2}, t_n + \frac{\Delta t}{2}\right)\Delta t$$
$$K4 = f(V_n + K3, t_n + \Delta t)\Delta t$$

Gill's version of 4th order R-K (R-K-G) method has the advantage of minimized rounded errors and storage requirements are reduced.

Both Euler and Runge-Kutta methods are explicit numerical integration methods for ODE and they have weak numerical stability with stiff systems. Stiffness is associated with the range of time constants used in the system model.

c) Trapezoidal Rule: 2nd order Trapezoidal rule is the simplest implicit integration method. It uses linear interpolation. The stiffness of the system being analysed affects the accuracy but not the numerical stability.

In the trapezoidal integration method the value of a variable is defined as a function of previous time step value and current time value. The equation is given by equation (2.13).

$$V_{n+1} = V_n + \frac{\Delta t}{2}[\, f(V_n, t_n) + f(V_{n+1}, t_{n+1})] \tag{2.13}$$

This method is numerically stable and has robust integration routine compared to other methods. Generally for systems involving simulation in which time steps are limited by numerical stability conditions rather than accuracy, implicit integration methods are better suited than explicit integration methods.

2.5 Power system simulation tools

Based on the power system phenomena and available mathematical analysing tools different power system simulation software packages are compared (all of them are time domain simulation software). PSS/E, DigSILENT, MATLAB (SimPowerSystem Simulink toolbox and PSAT toolbox) and RTDS are among the software packages to be compared.

2.5.1 Power Systems Simulation for Engineers (PSS/E)

PSS/E is an integrated, interactive program for simulating, analysing and optimizing power system performances. It can be used for the study of power system transmission network and generation performance in steady-state and dynamic condition like analysis of power flow, fault analysis and dynamic simulation events [1]. Hence PSS/E is not suitable for the study of electromagnetic transients which need a detailed model of power system components.

To implement the network model of a given power system in PSS/E, first one has to examine the physical components like transmission lines, generators, loads and control systems (excitation and governor). Then decide on the relevant equations and parameter values to be used. Finally, change these information into the form of a PSS/E input data file format (both in load flow data input file and dynamic data input file). PSS/E *Working file* contains different *Activities* (data input files, power system analysis functions and result output listing files). Once the appropriate information and parameters of the system are identified, the next step is to put these values to the *data input file Activity* using the text editor mode. Then it is possible to develop the graphical representation of the system. By selecting the desired mathematical analysis from the *Solution Activity* it is possible to see the response of the system using a *Reporting Activity*.

In PSS/E some components of a power system need to have equivalent circuit parameter representation to be implemented in the data input file, for example a three-winding transformer, otherwise it impossible to implement such components [1].

2.5.2 Digital Simulator for Electrical Network (DIgSILENT)

DIgSILENT Power Factory is a dedicated electrical power system simulation tool used by the power-system utilities [3]. DIgSILENT has the ability to simulate load flow, RMS simulations and electromagnetic transient events.

It provides models for different types of simulations: models for electromagnetic transient simulations on the bases of instantaneous values and models for electromechanical simulations on the bases of RMS values. This makes the models useful for studies of fast transient events during grid fault and long term power quality and control issues. For example, RMS simulation is more appropriate for long simulation periods by neglecting the electrical transients, as in the study of power system dynamic behaviour and power quality. On the other hand EMT simulation is useful for a simulation of the short period grid behaviour during faults.

DIgSILENT provides both a comprehensive library of models for electrical components in power system and a dynamic simulation language (DSL). Hence, there are two types of models in DIgSILENT, built-in and dynamic simulation language. Built-in models are standard electrical component models, already existing in the DIgSILENT library like generators, motors, controllers, dynamic loads and various passive network elements (such as lines, transformers, static loads and shunts). DSL models are models components created by the user with the help of dynamic simulation language. This makes it possible for users to create their own blocks either as modifications of existing models or as completely new models. These new models can be gathered in a library.

Finally, a given grid can be modelled in a graphical environment where the power system component models (built-in models) are dragged-dropped and connected.

2.5.3 MATLAB

Matlab is a high-level programming language for technical and engineering computations [4]. It combines programming, computation and visualization in an easy to use environment where problems and solutions are expressed in familiar mathematical notation and programming language coding. Typical uses include:

- Mathematical computation
- Modelling and simulation
- Data analysis, exploration and visualization
- Scientific and engineering graphics
- Application development, including graphical user interface building
- Simulink and State flow block-diagram graphical design environment

There are different Matlab based graphical toolboxes that can be used for power system analysis. Among these are SimPowerSystems (SPS) and Power System Analysis Toolbox (PSAT).

SimPowerSystems: is a modern design tool that allows scientists and engineers for rapidly and easily modelling, simulating and analysing power systems [4]. It uses Matlab as computational engine hence it is possible to use Matlab toolboxes during design and it can also support linear and nonlinear systems modelled in continuous time. During modelling a graphical user interface (GUI) can be used to build models as block diagrams by click-drag operations. With this interface, the desired dynamic systems can be easily built. SimPowerSystems operates in the Simulink environment hence it can include a comprehensive built-in block library of sinks, sources, linear and nonlinear components, and connectors in addition to the power system blocksets. Using S-Functions it is also possible to customize and create user-defined blocks. Models are hierarchical, so they can be built using both high-level and low-level modelling approaches. The system can be viewed at a high level, then double-click blocks to go down through the levels to see increasing levels of model detail.

The simulation speed of the system that contains different components, like generators, power electronics and transformers is significantly depend on the type of mathematical tool used to solve the algebraic and differential equations.

PSAT: is a Matlab toolbox for static and dynamic analysis and control of electric power systems [5]. Power flow routine and state variable initialization is the core of PSAT. Further it can perform the following analysis; continuation power flow (CPF), optimal power flow (OPF), small-signal stability analysis (SSSA), time domain simulation (TDS) and phasor measurement unit placement.

For accurate static and dynamic power system analysis, PSAT supports different component models for power flow data (bus bar type, transmission lines and transformers, generators, constant power loads), continues and optimal power flow (generator power reserve, power supply and demand bids and limits), switching operations (transmission line faults and transmission line breakers), measurements (bus frequency and phasor measurement units), loads (voltage dependent loads, frequency dependent loads and ZIP loads), machines (synchronous machines and induction motors), controls (turbine governors, AVR, PSS, over-excitation limiters and secondary voltage regulators) and regulating transformers (load tap changer with voltage or reactive power regulators and phase shifting transformers). Using the GUI future of PSAT it is possible to draw a one line network diagram, set system and routine parameters and plot results.

PSAT has Newton-Raphson and Fast Decoupled Power Flow iteration methods to solve algebraic equations and it uses Forward Euler method and Trapezoidal method to solve the differential algebraic equations.

2.5.4 The Real-Time Digital Simulator (RTDS)

This digital simulator is a special purpose computer, initially designed to study Electromagnetic Transient Phenomena in real-time [6]. The RTDS is a sophisticated

digital simulator both in computing hardware and detailed models of power system components, in other words it is hardware-software simulator. The RTDS hardware consists of different cards that contain the digital signal processors. While the software called RSCAD has a power system component model library and GUI environment to assemble a given network. Once the network is assembled, it should be compiled to map each component to the processors and to generate the low level machine langue for the Runtime module operation.

2.5.4.1 RTDS Hardware

RTDS hardware is Digital Signal Processor (DSP) based and utilizes advanced parallel processing techniques in order to reduce the computation burden for continuous real time operation. The RTDS hardware interacts with RSCAD software during the run-time and it performs all computations in real time. In order to realise and maintain the required real time computation, different racks can be utilized. Each rack has processing cards with digital and analogue I/O ports (triple processor card (3PC), RISC processor card (RPC), GIGA processor card (GPC)) and communication cards. All these cards are interconnected to each other using the common backplane to facilitate data exchange between individual processors and between racks.

The RTDS hardware in HCPS lab of Delft University of Technology contains 8 racks and each rack has 7*3PC, 1*RPC, 1*IRC and 1*WIC cards. In total there are 184 processors;

8*7*3 = 168 processors of 3PC type, and
8*1*2=16 processors of RISC type

Processing cards

1) **3PC:** each 3PC card contains 3 ADSP-21062 digital signal processors (they are also called shark processors) that are used to run the simulation. The number of power system and control system component models that can be included in the simulation is determined by the available number of these processors. The processors need 25 ns to perform each instruction cycle of a component model.

   In addition to the processors each 3PC card has analogue output channels, which can be used to monitor signals from the simulation. The digital input/output ports are also used for digital signal input/output for external equipment.

2) **RPC:** each RPC card contains 2 IBM PPC750CXe PowerPC processors. Unlike the 3PC processors RPC processors do not have input/output ports they are only used to solve the network during simulation. They need 1.67 ns to perform each instruction cycle of a component model.

3) **GPC:** each GPC card contains 2 IBM PPC750GX PowerPC processors. These GPC processors can be used to solve the network during simulation. Plus they have analogue output channels for signal exchange with external equipment. They need 1 ns to perform each instruction cycle of the component model, mostly these

processors are used for small time model of power system components that need small time steps up to 2.5 μs.

Communication cards

There are two communication cards; to that facilitate data exchange between racks and between racks and the work station computer.

1) **Inter-Rack Communications Card (IRC):** In multi-rack simulation cases the data exchange between processors residing on separate racks is accomplished through high speed communication channel mounted on the IRC. A single IRC card provides bidirectional data communication path from one rack to the other six racks.

2) **Workstation Interface Card (WIF):** In addition to IRC, each rack has one WIF card that facilitates the communication between the RTDS and the host computer workstation through ethernet cable based local area network. WIF do not have any effect on network solution, it regulates and facilitates data package exchange both between racks and between racks and the workstation computer during simulation.

2.5.4.2 RTDS software

In addition to the dedicated hardware the RTDS has user friendly GUI software called RSCAD. RSCAD has different Module/Activities for network assembly (Draft, Runtime, Transmission line and cable modelling modules) and it has also a library with a detailed component models. The RSCAD GUI module includes;

a) **Draft Module:** used for network assembly and data entry. In this module individual component icons can be selected from the library section and then placed on the network assembly section. The library of RSCAD has both power system and control block components under different groups.

b) **Runtime Module:** using this module it is possible to run a simulation and analyse the response of the simulation both in graph and meters. In addition to graphical view of signals, any control actions such as fault application or set point adjustment can be made dynamically in this module.

c) **Transmission line and Cable modelling modules:** used to enter the data of physical geometry and configuration of overhead transmission lines and underground cables.

2.5.4.3 RTDS Advantages and Limitations

Even though the RTDS has a capability of computing both in digital mode and real time, it has also some limitations. Of course most of these limitations are related to the available number of processors and the type of processors, some of the component models are processor type dependent.

Advantages

Since RTDS combines the real-time operating properties of analogue simulators with the flexibility and accuracy of digital simulation programs, there are many areas RTDS can be applied which were performed by analogue simulators [7].

1) Exchange of signals between the real world and the simulator like in protective relay and control equipment testing.
2) Interactive operations of the simulation by mouse click action.

Limitations

Even though the RTDS has a capability of computing both in digital mode and real time, it has also some limitations. Of course most of these limitations are related to the available number of processors and the type of processors, some of the component models are processor type dependent.

1) Trade off between number of processors and computation time. For a given number of processors as the size of the network increases, the computation burden of the processors also increases and there may be out of the real time operation mode. Plus in some cases two or three component models (either control block component models or some power system component models) can be assigned to a single processor while some power system component models need a single processor for one model only. So, the number of available processors must be larger than the number of power system components to be implemented. Thus, the size of the network to be implemented affects the real time computation capability of the simulator.

2) Limited flexibility in the data entry options of components.

3) In the case of using more than one rack lower limit of inter-rack communication time. The minimum time needed for inter-rack communication channel is a single time step, and a transmission line is used to establish this communication. Hence, the length of this transmission line is determined by the time step and the minimum length could be 15 km for 50 μs time step.

To summarise the above time domain simulation software packages based on their capability to analyse the interest of power system phenomena,

- PSS/E is used to analyse power system dynamic simulation and load flow.
- DIgSILENT is used to analyse EMT simulation, power system dynamic simulation and load flow calculation.
- SimPowersystem is used to analyse EMT simulation, power system dynamic simulation and load flow calculation.
- PSAT is used to analyse power system dynamic simulation and load flow calculation.
- RTDS is basically used to analyse EMT simulation but it can be also used in dynamic simulation and load flow calculation.

Except RTDS all the other software packages are non-real time simulation methods. According to [8] and the user manual of the above software packages, the following table summarises the comparison.

Table 1- 1: Comparison of simulation software packages

		PSS/E	DIgSILENT	SPS†	PSAT	RTDS
Component model	Generator model	3^{rd},5^{th}	7^{th}	7^{th}	3^{rd},5^{th}	7^{th}
	Generator saturation parameters	S1.0, S1.2	S1.0,S1.2	10 points on the OC curve	10 point on OC curve	S1.0,S1.2 or 10 points on OC curve
	Transmission line model	pi-model	pi-model, distributed line model	pi-model, distributed line model	pi-model, distributed line model	pi-model, distributed line model
	Static load model	Exponential and ZIP load	Exponential and ZIP load	ZIP load	ZIP load	Exponential and ZIP load
Solution methods	Load flow (iteration method)	Gauss-Seidel and Newton-Raphson	Newton-Raphson	Gauss-Seidel and Newton-Raphson	Gauss-Seidel and Newton-Raphson	Newton-Raphson
	Dynamic solution (numerical integration)	Fixed step trapezoidal	Variable step trapezoidal	Both Euler and fixed/variable step trapezoidal	Both Euler and fixed/variable step trapezoidal	Dommel-EMTP (trapezoidal)
	Simulation time step	user defined (>=10 ms)	user defined in μs or ms	user defined in μs or ms	user defined in μs or ms	user defined in μs
User interaction	Event definition and modelling	GUI and using C programming	GUI and using DPL or DDL	GUI and in Matlab programming and C	GUI and in Matlab programming and C	GUI using the library components
	Data input	GUI or text (data input file)	GUI input window	GUI or text	GUI or text	GUI input window
	Data output/display	graph/text	graph	graph/text	graph/text	graph
Simulation type	Electromagnetic transient	No	Yes	Yes	No	Yes
	Dynamic simulation	Yes	Yes	Yes	Yes	Yes

† SPS (SimPowerSystems)

Chapter 3

Implementation of Existing Noord-Holland Grid

3.1 Introduction

The existing grid of Noord-Holland will be implemented on the RTDS based on the available models in VISION and DIgSILENT. The grid to be implemented consists of 150 kV and 380 kV voltage level substations and 10 central generation units. In the given system there is a total active power load of 3409 MW and reactive power load of 1347 MVAr. Among this power demand, 1606 MW active power and 536 MVAr reactive power is generated by the central generators. All these generators are connected to the 150 kV substations via a transformer. The loads are aggregated to the 150 kV substations with corresponding summed-up active and reactive power. The Noord-Holland grid is connected to the rest National grid through a 380 kV substation at Diemen. As shown in Table 3- 1 the remaining 1803 MW active power and 747 MVAr active power is delivered by TenneT national grid via Diemen 380 kV infinite bus. Below Figure 3-1 shows the geographical view of Noord-Holland grid.

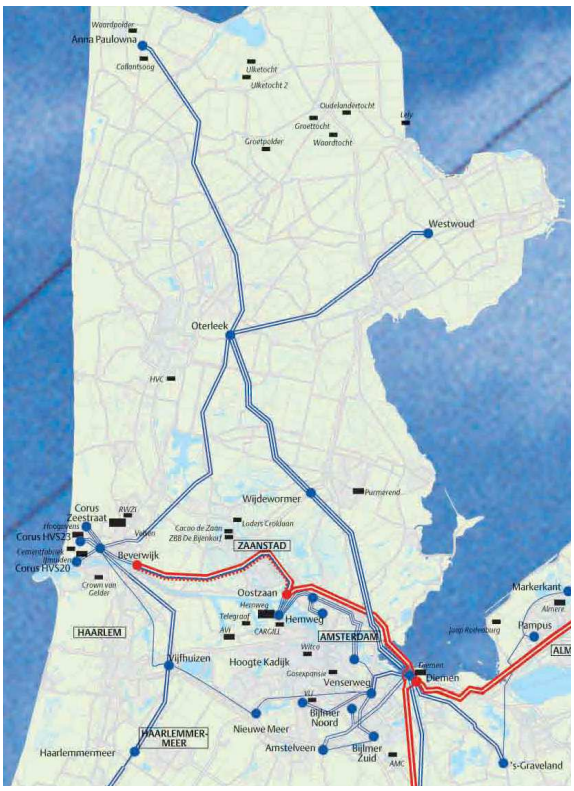

Figure 3- 1: Geographical location of Noord-Holland grid map: Red (380 kV) and Blue (150 kV) transmission lines.

In the present day power system the topology has a strong hierarchical structure. There are a few centralized large power plants that produce the power demand of consumers. The power flow is top-down from the power plants to the consumers.

Table 3- 1: Average generated power by the central Generators in Noord-Holland grid.

Central generators	S (MVA)	P (MW)	Q (MVAr)
HW-E8	692	650	238
VN25	421	360	132
IJM01	145	125	73
DM33	232	231	83
AVI-1	40	40	12
AVI-2	40	40	26
AVI-3	68	68	15
PU-1	64	63	2.5
HVCA	30	30	18
Total generated power		1606	600
TenneT		1803	747
Total load demand		3409	1347

Figure 3- 2 shows the simplified single line network diagram of 150 kV and 380 kV Noord-Holland grid.

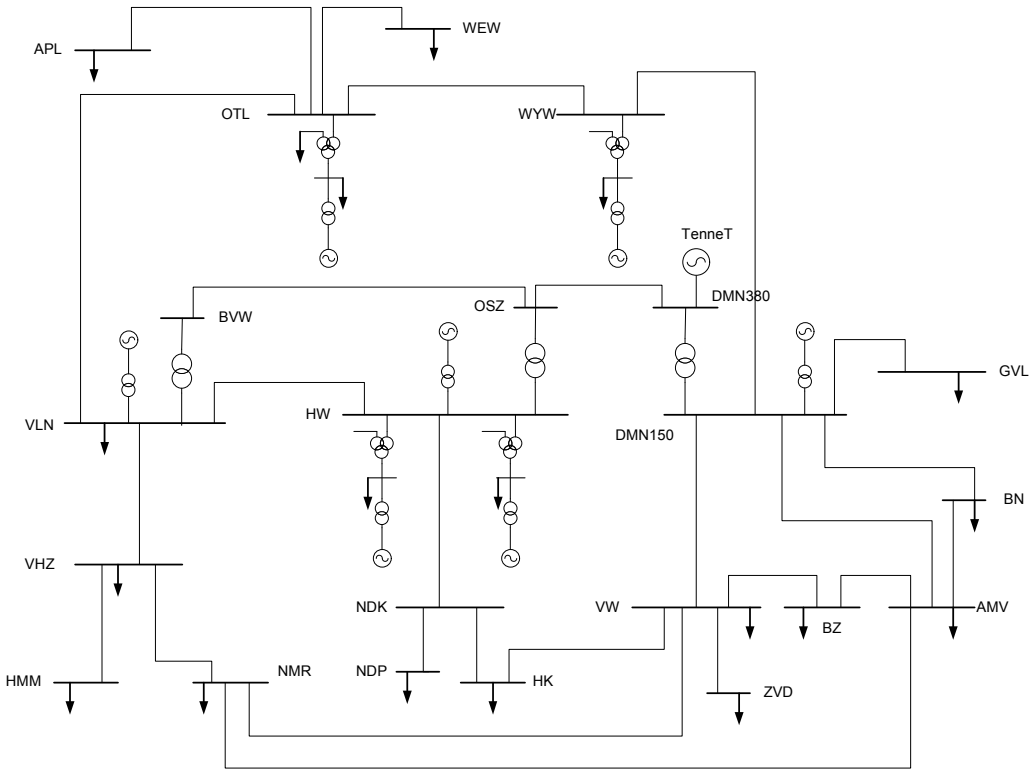

Figure 3- 2 : Simplified single line diagram of Noord-Holland grid model.

3.2 Modelling of the existing grid in RTDS

As explained in the previous chapter there is a trade-off between the number of power system components to be implemented and the number of available processors in RTDS hardware. As shown in
Figure 3- 2 the existing Noord-Holland grid consists of a large number of power system components so it is not possible to implement the whole grid in one rack of the RTDS. The following points are the main reasons to divide the grid into different racks:

- Computation time increases proportional to the size of the network and the minimum integration time step to be used for real time operation also increases.

- For real time computation the number of components assigned to each processor has to be balanced, for example a synchronous generator needs one processor while more than one control block components can be assigned to a single processor for a given time step.

To simulate the Noord-Holland grid in real time mode the network must be divided into different racks as shown below in Figure 3- 3.

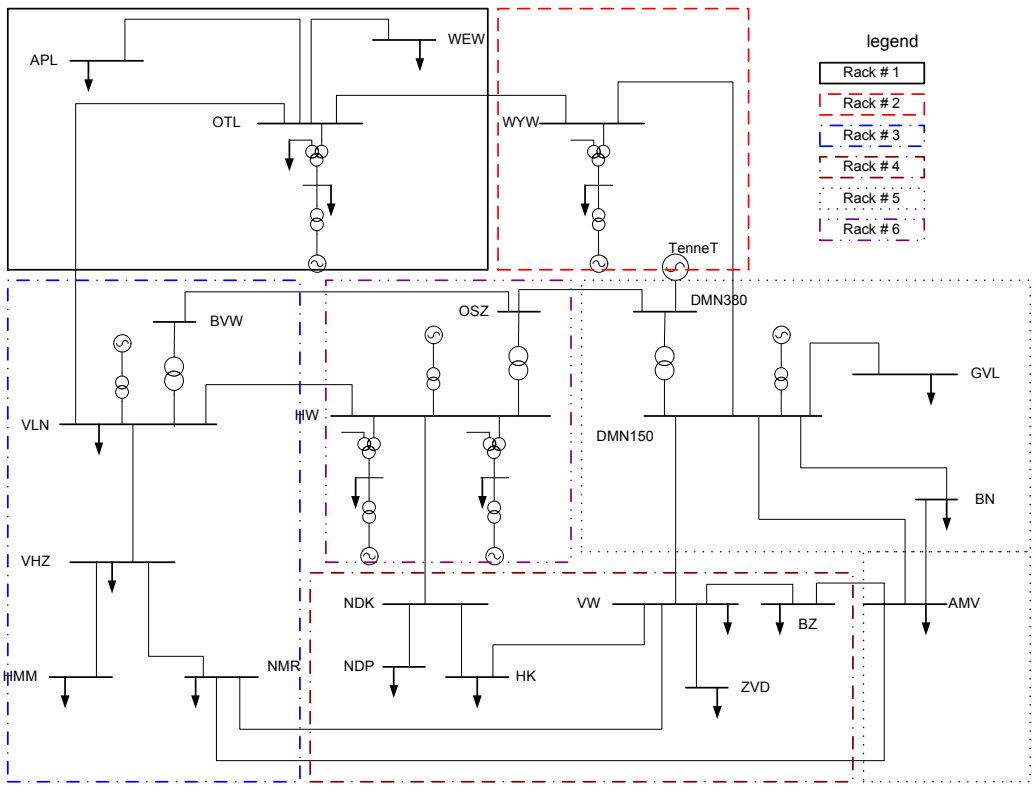

Figure 3- 3: Schematic division of Noord-Holland grid into different racks of the RTDS.

As the network is divided between different racks, it is necessary to have a real time data communication and exchange between these racks. To realise this, each rack has an Inter-Rack communication channel card that give the ability to communicate with other racks (maximum of six other racks).

To do this a transmission line has to be implemented, at least with a travel time equal to a single integration time step. For 75 μs integration time step, the travelling time of the transmission line that interconnects two racks must be greater than or equal 75 μs. For example for the speed of light, 300,000 km/s propagation velocity of the electromagnetic wave the length of the line must be greater than or equal to 22.5 km.

Generally, the propagation velocity of an electromagnetic wave through a transmission line or a cable depends on the inductance and capacitance values. For a given values of L and C, the propagation velocity of the electromagnetic wave is given by:

$$v_p = \sqrt{\frac{1}{LC}} \; ; \quad \text{where } v_p \text{ is propagation velocity in m/s} \tag{3.1}$$

Therefore, the travelling time of the electromagnetic wave is give by:

$$t_p = \sqrt{LC} \; ; \quad \text{where } t_p \text{ is travelling time in seconds}$$

For the implementation of the existing Noord-Holland grid in RTDS, the lines shown in Table 3- 2 are used as interconnecting transmission lines. For the real time simulation of Noord-Holland grid implemented in RTDS the minimum computation time required is 75 μs. Hence the integration time step must be greater than 75 μs. However, the travelling time for some of the lines is shorter than the required integration time step of 75 μs.

For those lines whose travelling time is shorter than 75 μs, their inductance (L) and capacitance (C) values are adjusted to result in a travelling time of 75 μs. After this adjustment the original line length has increased by some factor. This causes a change in the line impedance and current flow magnitude and direction. So it is not possible to say this model has the same network parameters as that of the actual Noord-Holland grid.

Table 3- 2: lines used for interconnecting different racks

Transmission line name	Travelling time $t_p = \sqrt{LC}$ in μs	Original line Length in km	Line length in km, t_p = 75 μs	Between Racks of
BVW-OSZ-ZW	35.63	15.94	33.56	#3 and #6
DMN-VW-WT	39.40	4.40	8.38	#4 and #5
DMN-VW-ZW	39.40	4.40	8.38	#4 and #5
AMV-BZ	46.78	5.975	9.58	#4 and #5
DMN-OSZ-ZW	51.72	15.94	23.12	#3 and #5
DMN-OSZ-WT	51.72	15.94	23.12	#3 and #5
OTL-WYW-ZW	53.39	15.26	21.44	#1 and #2
OTL-WYW-WT	53.39	15.26	21.44	#1 and #2
OTL-WYW-GS	53.39	15.29	21.44	#1 and #2
HW-NDK-PS	55.67	6.30	8.49	#4 and #6
HW-NDK-ZW	55.67	6.30	8.49	#4 and #6
HW-NDK-WT	55.67	6.30	8.49	#4 and #6
AMV-NMR	94.51	9.924	N/A	#3 and #5
NMR-VW	112.22	12.799	N/A	#3 and #4
DMN-WYW-WT	198.84	22.28	N/A	#2 and #5
DMN-WYW-GS	198.84	22.28	N/A	#2 and #5
DMN-WYW-ZW	198.84	22.28	N/A	#2 and #5
OTL-VLN-ZW	253.60	25.61	N/A	#1 and #3
OTL-VLN-WT	253.60	25.47	N/A	#1 and #3
HW-VLN-WT	284.52	24.686	N/A	#3 and #6

In addition to real time simulation it is also possible to do non-real time simulation. In the case of non-real time simulation the integration time step of the simulation can be adjusted. During a non-real time simulation the integration time step can be equal to the travelling time of the shortest interconnecting transmission line while the minimum computational time required for each integration time step remains the same as the real time simulation. For non-real time simulation, the integration time step can be reduced to 35 μs (equal to travelling time of BVW-OSZ-ZW) while the computational time for each integration time step remains 75 μs (minimum computational time required). So for non-real time simulation, there is no need to adjust the travelling time of the lines and hence the line impedance remains the same as the original value. The non-real time simulation will be used to validate the RTDS model.

Once the network has been divided into different racks, the next step is to implement each power system component and the necessary control blocks using the Draft module of RSCAD as shown below in Figure 3- 4.

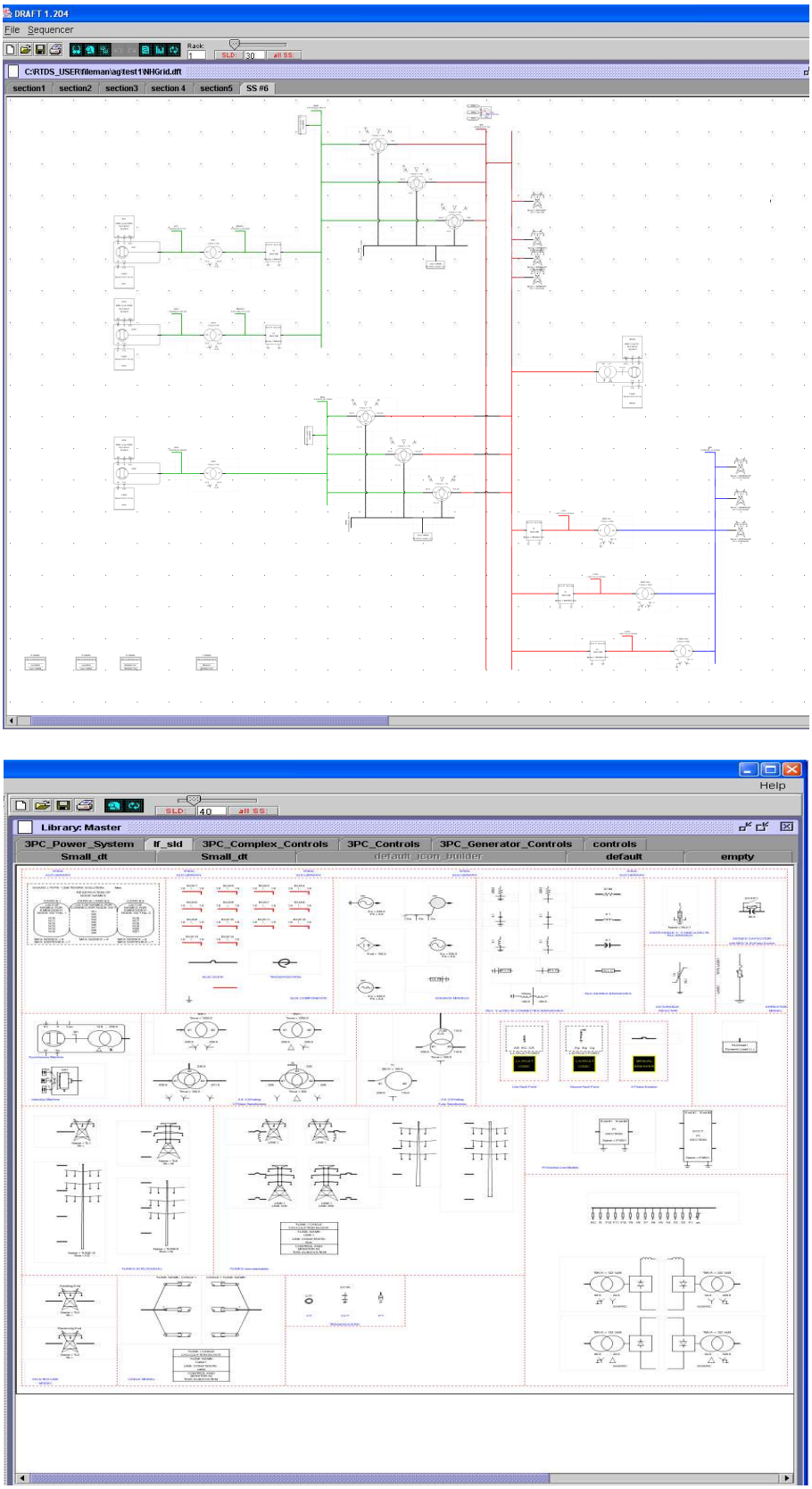

Figure 3- 4: Above Draft module and below library of RSCAD respectively.

The Draft module of RSCAD is used to assemble the network by interconnecting the component models from the library. In the following, the description of the power system component models in the RSCAD library is given.

Synchronous generator

In the RSCAD library the available synchronous generator model uses either the fundamental or operational parameters. For most of the generators the available data is in dq axes parameters hence all generators are modelled using the dq axes parameters.

The model of the synchronous generator in RSCAD needs sub-transient and transient parameters, i.e. it is a 7^{th} order model. In the DIgSILENT model of Noord-Holland grid the sub-transient and transient values of all the generators are available in dq axes reference. All used parameters of the synchronous generators are available in Appendix C.

Controls of Generators

In RSCAD all possible IEEE standard generator control systems are available. For excitation control there are different models like; EXAC types, EXST types, EXDC type, EXPIC type, IEEET and IEEEX types. As mentioned in [10] all the generators are equipped with the appropriate excitation control system. All the controls block diagrams and parameter values are shown in Appendix B.

For the governor control there are also standard control models in RSCAD. Under this group there are gas turbine governor, hydro turbine governor, steam turbine governor and IEEE standard governors. Similar to the excitation controls, the block diagrams and parameters of these controls are available in Appendix B.

2-winding 3-phase Transformer

The required data of 2-winding 3-phase transformer are nominal power, Voltage ratio, leakage reactance and no-load loss. All these data are available in both VISION and DIgSILENT models. The leakage reactance can be derived from the short circuit voltage and the iron loss data. The parameters of the 2-winding 3-phase transforms are listed in Appendix C.

3-winding 3-phase Transformer

For 3-winding 3-phase transformer model except the leakage reactance all the data is directly available in the DIgSILENT model. The leakage reactance can be calculated from the short circuit voltage percentage and the iron loss of the windings.

According to [3] the leakage reactance between two windings can be calculated as shown in Equation(3.2).

$$u_{r,SC,HV-MV} = \frac{P_{cu,HV-MV}}{Min(S_{rT,HV}, S_{rT,MV}) \cdot 1000} \cdot 100\%$$

$$u_{i,SC,HV-MV} = \sqrt{u^2_{SC,HV-MV} - u^2_{r,SC,HV-MV}}$$

$$x_{\sigma,HV-MV} = \frac{u_{i,SC,HV-MV}}{100\%} \tag{3.2}$$

where $u_{r,SC,HV-MV}$ real part of the short-circuit voltage HV-MV in %

$u_{i,SC,HV-MV}$ imaginary part of the short-circuit voltage HV-MV in %

P_{cu} copper loss in kW

$S_{rT,HV}$ rated power of HV winding in MVA

$S_{rT,MV}$ rated power of MV winding in MVA

This calculation is repeated for each pair of windings. The parameter of leakage reactance for each transformer is available in Appendix C.

Loads

In RSCAD library all possible load model types are available; passive RLC, ZIP, exponential ZIP and dynamic loads. For the implementation of all the loads in Noord-Holland grid, the constant active and reactive power load model is used.

The set-point for this load model can be controlled or varied during the Runtime module using sliders; this helps to see the effect of load variation easily. The active and reactive loads connected to each substation are shown in Appendix C.

Transmission line

There are two types of transmission line models; travelling wave transmission line model and PI section models. Both of these models are available in RSCAD.

For a travelling wave transmission line model there is a separate data entry module in RSCAD. In this module it is possible to enter either physical parameter data or equivalent RLC values.

For the physical parameter data entry option the user needs to enter all the necessary data like, rated voltage and current, conductor radius, tower height and DC resistance of the conductors. For equivalent RLC option the user needs to enter the positive and negative sequence RLC values per km and the total length of the line.

The travelling wave transmission line model is used to implement an interconnection channel between two racks and it can also be used within a rack as long as the travelling time is greater than a time step.

For travelling time of less than a time step the transmission line model is implemented by the PI section line model. PI section model is used only within a rack. In PI section model, the user needs to enter the positive and negative sequence equivalent RLC parameters.

Voltage source

The voltage source model is used as an infinite source (to represent the external grid) to balance the active and reactive power flow. Plus it is connected to the slack bus to keep the magnitude and the phase angle of the voltage at the reference value; for example 1.0 pu at $\angle 0^0$.

The external grid is implemented using a voltage source with a positive sequence reactance determined by the maximum short-circuit current at that connection point. According to the VISION model the negative sequence reactance is the same as that of the positive sequence. The positive sequence reactance is derived from the ratio of nominal voltage and maximum short-circuit current.

The reference voltage at the connection point to the national grid, at Diemen 380 kV, is 1.05 pu, this means the voltage level at this substation is 400 kV. In RTDS model all the substations of 380 kV had to be implemented as 400 kV substations for consistency.

Runtime module of RSCAD

Once the network has implemented successfully the next step is to compile the Draft file. During compilation a low level machine language code is generated and the components are assigned to the available digital signal processors.

After a successful compilation the Runtime module can be opened. On the right side of the Runtime module GUI environment all online racks should be available with red indicators.

Using the Runtime module of RSCAD different actions can be applied and graphs and meters can be used to see the response of these actions.

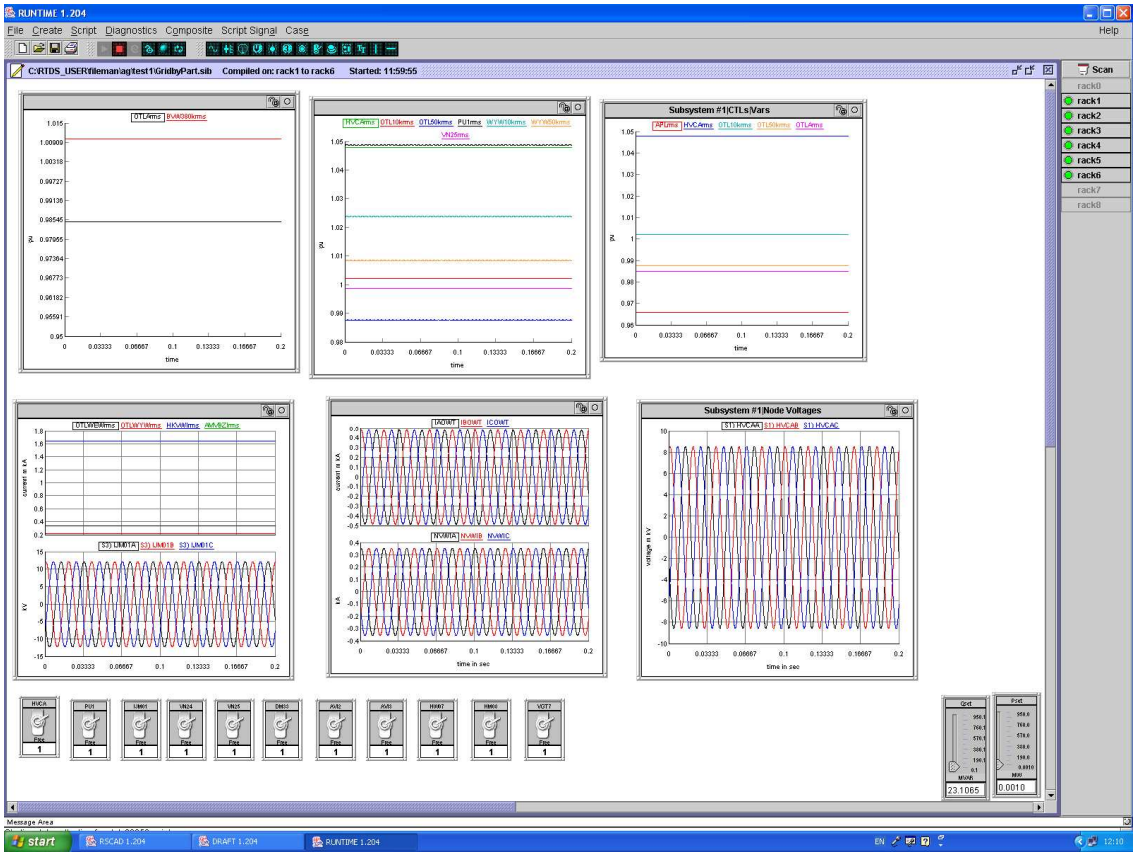

Figure 3- 5: Runtime module of RSCAD.

3.3 Validation of the model

To validate this model a comparison is done with the VISION and DIgSILENT models. The load flow values of RTDS and VISION are compared. For the dynamic behaviour the comparison is done with the DIgSILENT model.

3.3.1 Steady State value validation

In order to verify the implemented model of Noord-Holland grid in RTDS, a load flow value comparison has been done with the VISION model. Both network models are the same.
In Table 3- 3 the load flow node voltage values for both RTDS and VISION models are shown. In addition to the node voltages, the currents through the lines are also shown in the Appendix A.

Table 3- 3: load flow value comparison between RTDS and VISION

Substation Name	Unom	U [pu]		angle [degrees]		U_% error	angle % error
	kV	*RTDS*	*VISION*	*RTDS*	*VISION*		
Velsen	150	0.996	1.003	-8.969	-8.495	-0.70%	5.58%
Anna Paulowna	150	0.981	0.983	-14.225	-13.484	-0.20%	5.50%
Wijdewormer	150	1.012	1.014	-9.790	-8.973	-0.20%	9.11%
Noord Klaprozenweg	150	1.004	1.000	-3.847	-3.618	0.40%	6.33%
Hoogte Kadijk	150	1.002	0.998	-3.978	-3.750	0.40%	6.08%
Venserweg	150	1.033	1.036	-7.604	-6.768	-0.29%	12.35%
Bijlmer Zuid	150	1.031	1.034	-7.715	-6.902	-0.29%	11.78%
Amstelveen	150	1.031	1.034	-7.733	-6.991	-0.29%	10.61%
Vijfhuizen	150	0.998	1.006	-9.591	-9.288	-0.80%	3.26%
Haarlemmermeer	150	0.993	1.002	-10.104	-9.793	-0.90%	3.18%
Bijlmer Noord	150	1.034	1.037	-7.261	-6.660	-0.29%	9.02%
Oterleek	150	0.999	1.002	-11.535	-10.808	-0.30%	6.73%
Diemen	150	1.038	1.041	-6.951	-6.045	-0.29%	14.99%
s-Graveland	150	1.027	1.029	-8.062	-7.149	-0.19%	12.77%
Hemweg	150	1.006	1.002	-3.615	-3.384	0.40%	6.83%
Nieuwe Meer	150	1.028	1.031	-7.959	-7.207	-0.29%	10.43%
Westwoud	150	0.985	0.987	-13.283	-12.546	-0.20%	5.87%
Diemen	380	1.053	1.053	0.000	0.000	0.00%	0.00%
Oostzaan	380	1.051	1.051	-0.405	-0.483	0.00%	-16.15%
Beverwijk	380	1.050	1.050	-0.891	-0.947	0.00%	-5.91%

As shown in Table 3- 3 the load flow results from RTDS are more or less similar to the VISION load flow result. The load flow voltage difference between RTDS and VISION model is less than 1.0%. Even this difference could be the result of the way how the load flow equations are solved by the software.

3.3.2 Dynamic behaviour response validation

In this part the dynamic behaviour comparison between RTDS and DIgSILENT models is done. For the dynamic behaviour comparison a short-circuit test is performed at four different substations in both models. For the purpose of validation with the DIgSILENT model all generators are not equipped with any control system during these tests. They have only constant excitation voltage and constant input mechanical torque.

Test One: Short-circuit test at Diemen 150 kV

For this short-circuit simulation, a fault with a 4 Ω grounding resistance and duration of 600 ms is applied at Diemen 150 kV substation. The simulation results from both RTDS and DIgSILENT models are shown in Figure 3- 6. Even though the voltage dips during a fault are comparable, the post-fault responses are not exactly the same. In RTDS model the oscillation is small but the rise time of the voltage after clearing the fault is longer. However, the general response behaviour is comparable in both models as shown in Figure 3- 6.

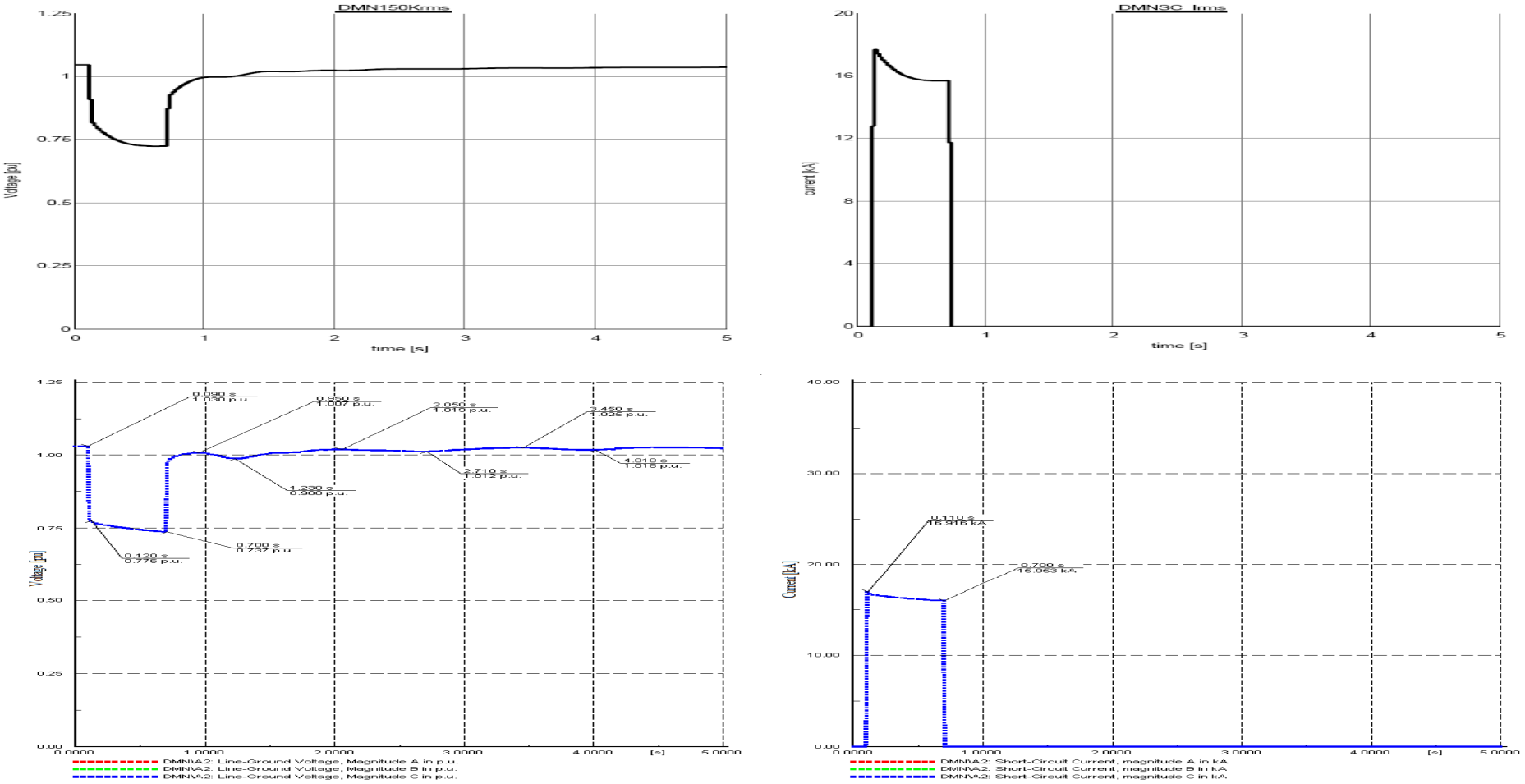

Figure 3- 6: 3-phase to ground fault response at Diemen 150 kV, RTDS model above and DIgSILENT model below respectively. The graphs on the right side are pu voltages and on the left side short-circuit currents in kA.

Test two: Short-circuit test at Westwoud 150 kV

At Westwoud 150 kV substation a short-circuit fault with 4 Ω grounding resistance and duration of 600 ms is applied. During this short-circuit fault the voltage drops to 0.35 pu. As shown in Figure 3- 7 the post-voltage oscillation behaviour of the voltage response is not still exactly the same as the DIgSILENT model but they are comparable. The magnitude of the short-circuit currents are almost the same.

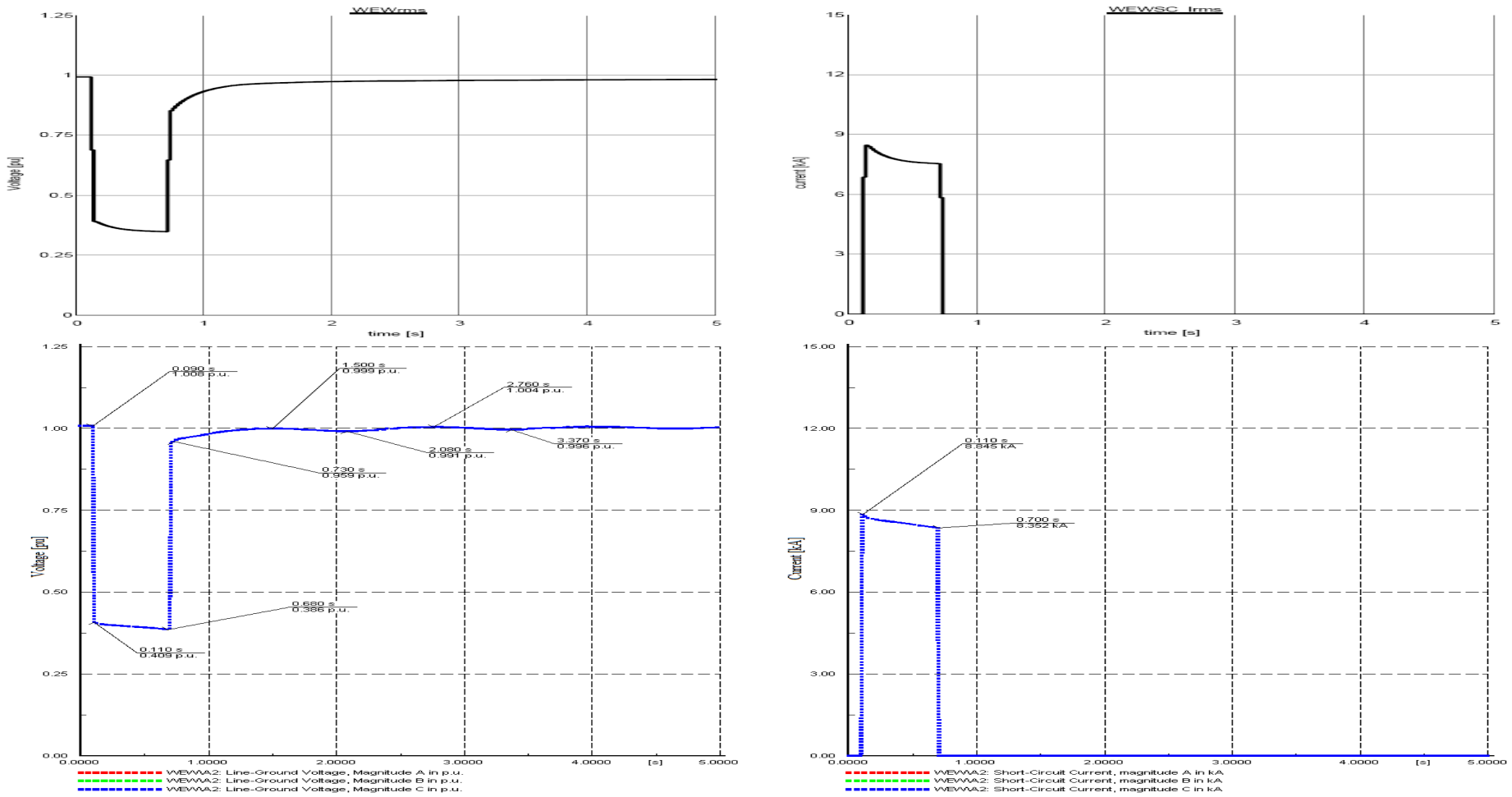

Figure 3- 7: 3-phase to ground fault response at Westwoud 150 kV, RTDS model above and DIgSILENT model below respectively. The graphs on the right side are pu voltages and on the left side short-circuit currents in kA.

Test three: Short-circuit test at Noord Klaprozenweg 150 kV

During a 3-phase to ground fault with 4 Ω resistance and 600 ms duration the behaviour of the voltage response is shown by Figure 3- 8. At this substation the post-fault voltage response shows large oscillations compared to previous substations. This happened because there are generators in the nearby Hemweg 150 kV substation. This oscillation is the reflection of the generator rotor oscillation because the frequency of the oscillation is in the range of 1 Hz. As shown in Figure 3- 8 the behaviour of the voltage response after clearing the fault is almost the same for both RTDS and DIgSILENT models. The short circuit current is a little bit smaller for RTDS model.

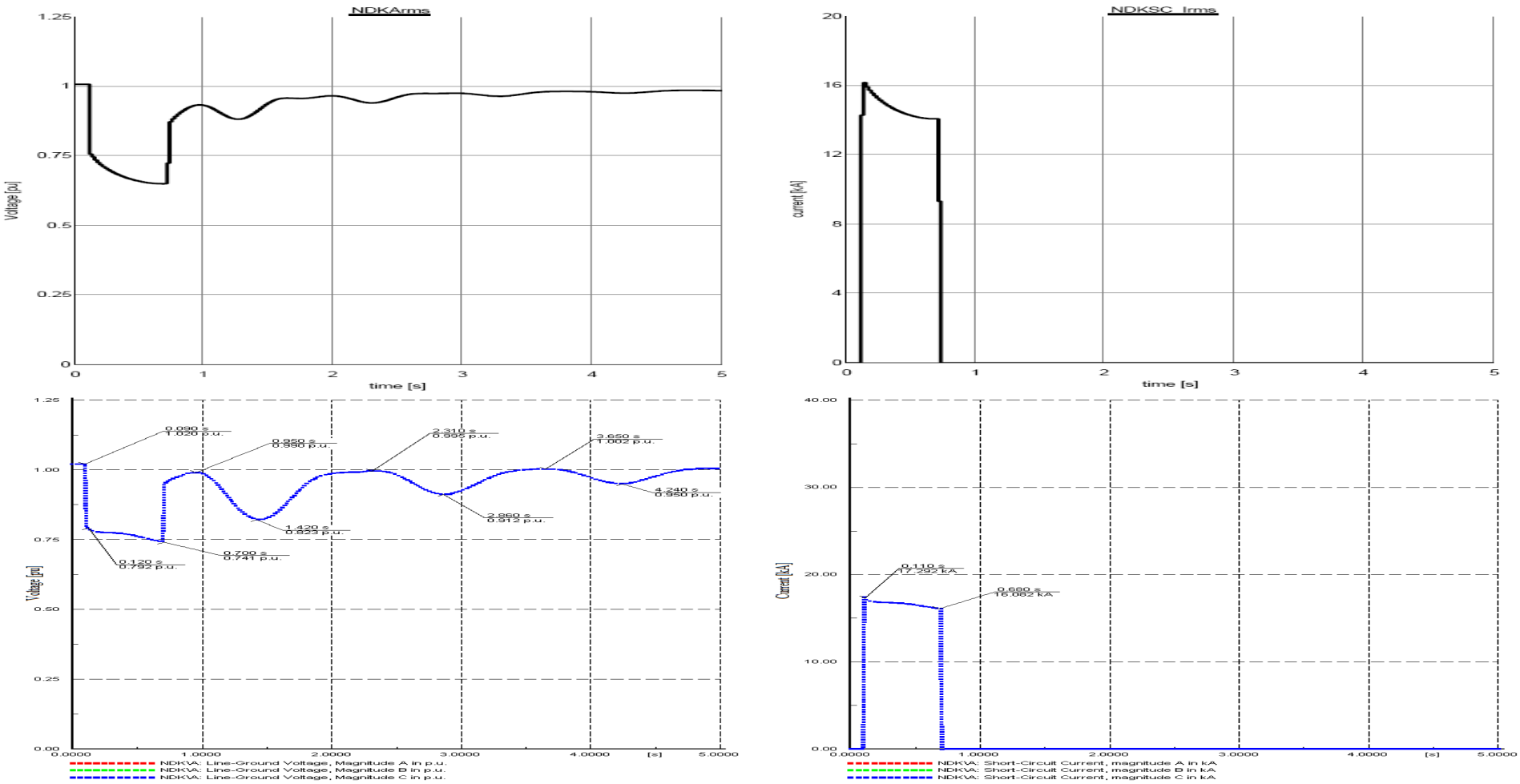

Figure 3- 8: 3-phase to ground fault response at Noord Klaprozenweg 150 kV, RTDS model above and DIgSILENT model below respectively. The graphs on the right side are pu voltages and on the left side short-circuit currents in kA.

Test four: Short-circuit test at Velsen 150 kV

The voltage response at Velsen 150 kV substation during a 3-phase to ground fault with 4 Ω resistance and 600 ms duration is shown in Figure 3- 9. The RTDS model gives less oscillation response compared to the DIgSILENT model. Even in the DIgSILENT model the oscillation damps faster for this test case than the other test cases. Here again the magnitude of the short-circuit current for the RTDS model is smaller.

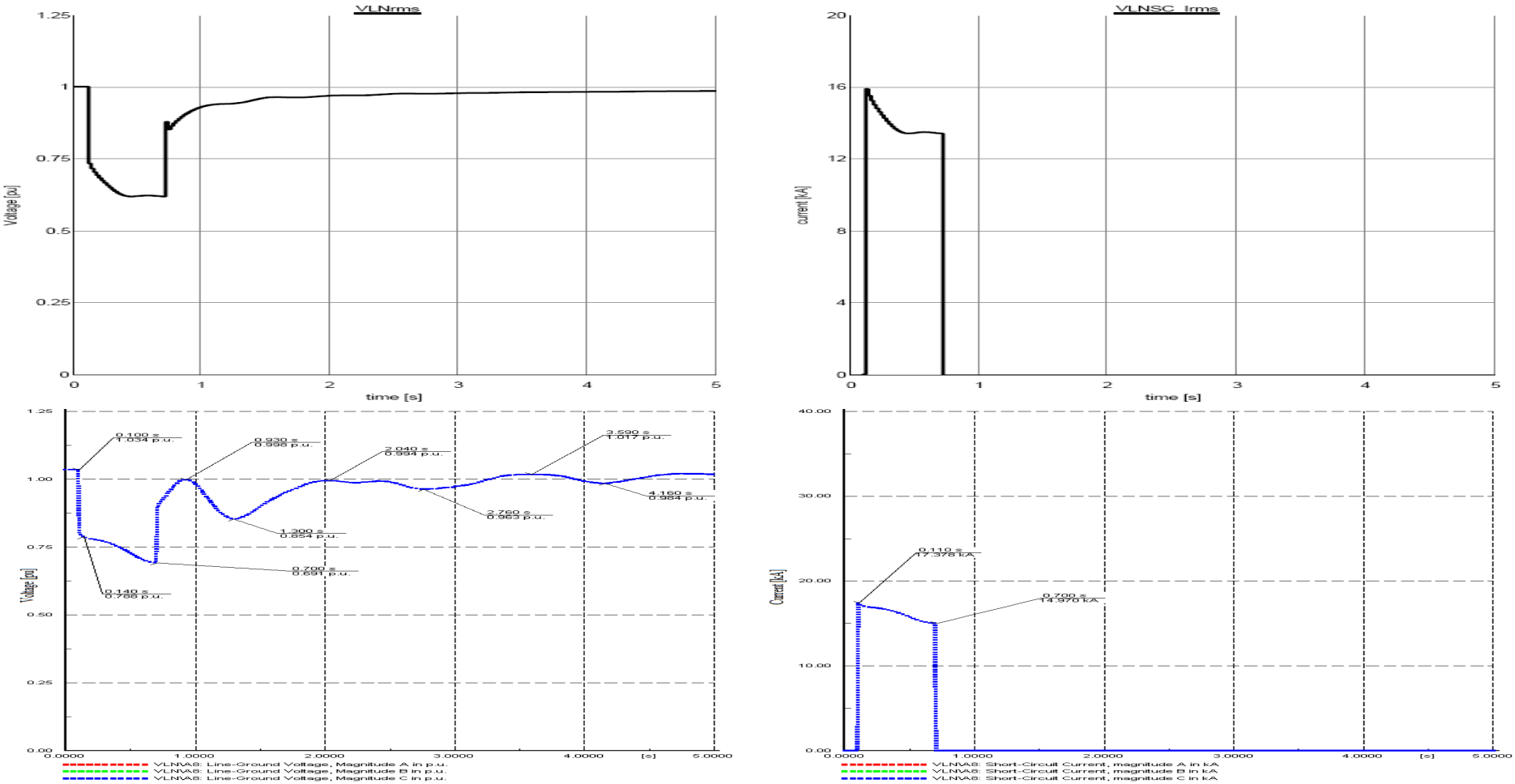

Figure 3- 9: 3-phase to ground fault response at Velsen 150 kV, RTDS model above and DIgSILENT model below respectively. The graphs on the right side are pu voltages and on the left side short-circuit currents in kA.

At last the following points summarise the dynamic behaviour comparison between the RTDS and DIgSILENT models of Noord-Holland.

- The voltage response from the RTDS model shows less oscillation magnitude.
- For the RTDS model the oscillation damps faster.
- RTDS model gives smaller voltage rise just after the fault cleared.
- Generally the two models have comparable dynamic responses.

Below Table 3- 4 shows the percentage error from the numerical value comparison of voltage and short-circuit current just after the fault and just before clearing the fault.

Table 3- 4: Percentage error between the RTDS and DIgSILENT models for the voltage and short-circuit current.

150 kV substations	Voltage		Short-circuit current	
	JAF	JBCF	JAF	JBCF
Westwoud	4.90%	10.40%	4.10%	9.60%
Velsen	6.70%	10.10%	8.30%	9.80%
Noord Klaprozenweg	5.10%	12%	6.60%	12.30%
Diemen	5.40%	1.40%	4.40%	1.60%

* JAF →just after the fault

* JBCF →just before clearing the fault

As shown in Table 3- 4 the average error for the voltage and the short-circuit current is around 10%.

Chapter 4

Expansion of Existing Noord-Holland Grid to a Future Scenario

This chapter discusses the future extensions on the Noord-Holland grid. The future grid scenario will be developed by expanding the current grid of Noord-Holland with large wind power plant. The chapter starts by describing the future grid scenario. The available wind turbine technologies are also discussed. After that the possibilities to model these wind turbine generators in the RTDS is discussed. Last, the way how to develop the future grid with large wind power plant is discussed. Test results with large installed wind power are shown finally.

4.1 Future grid scenario

According to [10] in 2007 there were 94 GW installed wind power worldwide and among this the share of Europe was 61%. The average annual growth rate was 25%. This shows each year a huge amount of wind power is connecting to the grid.

According to the goal of the Dutch government the capacity of the off-shore wind power in the Netherlands will be increased to 6 GW by 2020 [9]. To achieve this goal there are three scenarios outlined about the growth of off-shore wind power. One of these scenarios is the called *Basic Scenario;* according to this scenario the growth rate of the installed wind power is equal from 2008 to 2020.

According to the TSO of Noord-Holland grid [Liandon], without a major upgrade of the existing grid it is possible to install only 3 GW power of micro-CHP and wind generation. From the micro-CHP it is expected each household in Noord-Holland will have 1 kW average output power. Assuming there will be about 1 million households in Noord-Holland; this gives about 1 GW total power from micro-CHP. So the remaining 2 GW power is assumed to be generated by off-shore wind farms.

Based on the *Basic Scenario* of the wind power installation growth, there will be around 0.167 GW power growth each year from 2008 to 2020 in Noord-Holland region. For example in 2015 the installed wind power will be around 1.2 GW. For the connection to the grid Beverwijk 150 kV is the proposed location in Noord-Holland region.

4.2 Wind turbine technology

In a wind farm there are a number of individual wind turbines interconnected to each to form small groups. These small groups also interconnected to form the large wind

farm. Based on the technology used, there are different types of wind turbines in the market.

There are two categories of wind turbines based on the operating speed behaviour of the machine used: fixed speed wind turbine and variable speed wind turbine.

Fixed speed wind turbines operate within very small range of mechanical speed. Squirrel cage induction generator (SCIG) is classified under this category.

Variable speed wind turbines operate within a wide range of mechanical speed. Under this category there are two types of wind turbine: double fed induction generator (DFIG) and full converter synchronous generator (FCSG). Both of these turbine types are equipped with a power electronic converter that converts the generator side frequency to a grid frequency.

According to the distribution of turbine technology [10], DFIG will be the most dominant wind turbine in the future market. The main reason for this dominance is:

- ✓ DFIG operates in wide range of speed compared to SCIG.
- ✓ The power rate of a power electronic converter used for DFIG is small fraction (around 25%) of the generated power compared to FCSG.

Both DFIG and FCSG are able to supply some amount of reactive power in addition the active power from the wind. Hence, from grid stability point of view they help for fast recovery of node voltage after clearing a fault [10].

4.2.1 Models of wind turbine

According to [10] there are three types of models for the representation of wind turbine in power systems. These models are: squirrel cage induction generator, double fed induction generator and direct drive synchronous generator. All these turbine models use the mechanical torque input from the wind to generate the electric power. When there are a lot of wind turbines on the same location they can be aggregated into a single wind farm model for power system simulation.

Aerodynamic behaviour of wind

The kinetic energy of the wind is converted to a useful and accessible electric power with the help of wind turbines. As the wind blows through the turbines, it loses some of the potential kinetic energy. This energy is used to drive the shaft of the turbines. The aerodynamic power extracted from the wind is described by the following equation:

$$P_w = \frac{1}{2} A \rho V_w^3 \tag{3.3}$$

Where, A = area swept by rotor blade in the direction of the wind.

ρ = air density

V_w = wind speed

Practically it is not possible to extract all kinetic energy of the wind. The maximum possible efficiency of the wind energy conversion is around 59%. So, the above equation is modified with the power coefficient term C_p.

$$P_w = \frac{1}{2} A \rho V_w^3 C_p(\lambda, \theta) \tag{3.4}$$

Where, $C_p(\lambda, \theta)$ = power coefficient

$\lambda = \frac{r\omega_m}{V_w}$: tip speed ratio; ω_m = mechanical speed of the generator

θ = blade pitch angle

The mechanical torque input to the generator rotor shaft is the ratio of wind power captured divided by the mechanical speed of the generator. As shown in equation (3.5) it is possible to control the instantaneous torque input to the generator using the tip speed ratio and the power coefficient.

$$T_m = \frac{P_w}{\omega_m} = \frac{\frac{1}{2} A \rho V_w^3 C_p(\lambda, \theta)}{\omega_m}$$

$$= \frac{1}{2} A \rho r V_w^2 \frac{C_p(\lambda, \theta)}{\lambda} \tag{3.5}$$

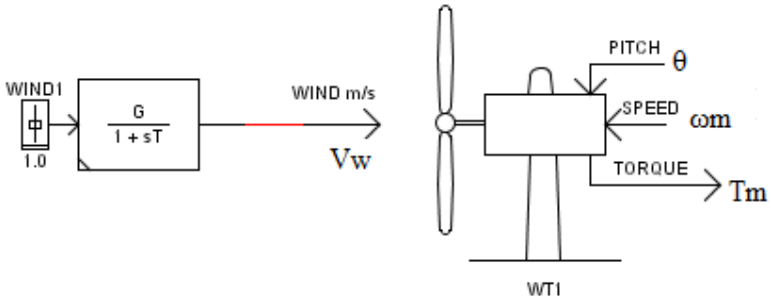

Figure 4- 1: Wind turbine model in RSCAD. The inputs to the turbine are wind speed (m/s), pitch angle of blade (degree) and mechanical speed of the generator (pu). The output is mechanical torque in pu. (Source [6])

For constant speed wind turbines the power coefficient C_p depends only on the ratio between the linear speed of the tip of the blade with respect to wind speed, λ and not on the pitch angle of the blades [11]. Thus, C_p is defined as a function of λ only.

$$C_p(\lambda) = 0.44\left(\frac{151}{\lambda_i} - 13.2\right)e^{\frac{18.4}{\lambda_i}}$$
$$\text{where, } \lambda_i = \frac{1}{\frac{1}{\lambda} - 0.003} \tag{3.6}$$

On the other hand, for variable wind turbines the power coefficient depends on both tip speed ratio and pitch angle of the blades. As shown in equation (3.7) the mechanical torque of wind turbine is mainly controlled by the wind speed, pitch angle and operating mechanical speed of the generator.

$$C_p(\lambda,\theta) = \left(0.044 - 0.0167\theta\right)\sin\left[\frac{\pi(\lambda-3)}{15-0.3\theta}\right] - 0.00184(\lambda-3)\theta \tag{3.7}$$

Squirrel Cage Induction Generator (SCIG)

The squirrel cage induction generator is one of the basic models of wind turbines. This induction generator supply electric power at grid frequency and it is possible to connect it directly to the grid. The operating speed of SCIG is always close to the synchronous speed, within the range of 1% to 2% above the synchronous speed. This is why SCIG categorised under a fixed speed wind turbine type generator.

According to the aerodynamic model of wind turbines, the instantaneous mechanical input torque, that is needed to drive the induction generator at mechanical speed ω_m, is controlled by the power coefficient C_p and tip speed ratio λ. This type of operating speed control is called passive stall control [11].

The drawback of SCIG type wind turbines is that they always consume a considerable amount of reactive power. Therefore, reactive power compensation mechanism such as a capacitor bank as shown in Figure 4- 2 should be included at the terminal of the generator. Using this reactive power compensation it is possible to operate close to unity power factor.

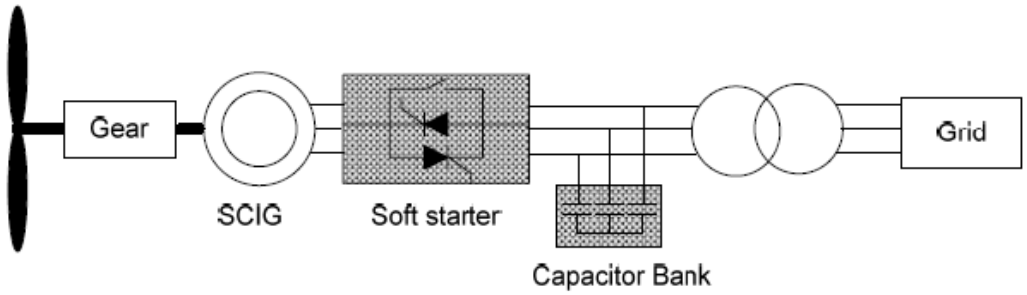

Figure 4- 2: Grid connected SCIG. (Source [12])

Double Fed Induction Generator (DFIG)

The DFIG is a variable speed wind turbine. The rotor windings of this generator are accessible through the slip rings. Hence, it is possible to control the rotor winding voltage both in magnitude and frequency [10]. As shown in Figure 4- 3 the rotor winding of DFIG is connected to the grid using a power electronic converter. The power electronic uses a PWM to control the frequency of the rotor winding in relation to the grid frequency.

The rating of this power electronic converter is only a small fraction of the total power generated by the wind turbine. So, the dimension of the converter is small compared to the full converter system.

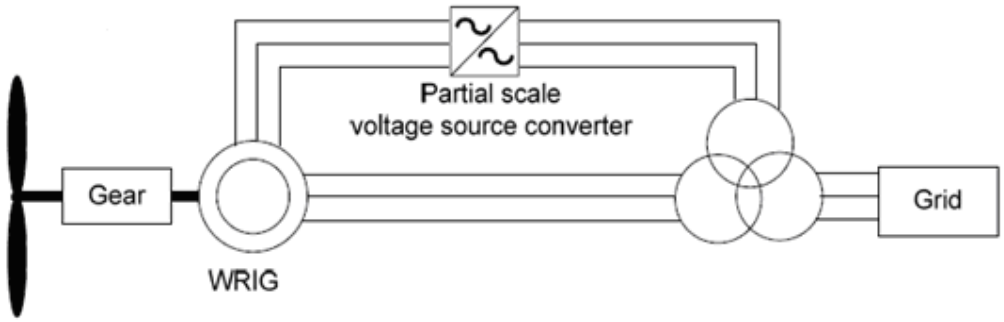

Figure 4- 3: Wound rotor induction generator with a VSC on the rotor side (DFIG). (Source [12])

For DFIG the power extracted from the wind is controlled by both: tip speed ratio and pitch angle of the turbine blade. This type of approach to control the aerodynamic efficiency is called pitch control [11].

Fully Controlled Synchronous Generator (FCSG)

A fully controlled synchronous generator is a variable speed wind turbine. This model consists of a synchronous generator and a full scale voltage source converter. The generator can use either excitation winding or a permanent magnet. In the case of a permanent magnet, it is hard to control the reactive power generated by the synchronous generator and permanent magnet machine is more expensive than other machine types.

Synchronous generator with an excitation winding is mostly used. In this case the reactive power generation is governed by the grid side converter while the active power is determined by the mechanical power coming from the turbine.

Since FCSG uses a full scale converter it is possible to use any type of electrical machine in addition to a synchronous generator. The grid side converter converts the generator side frequency to the basic grid frequency. Figure 4- 4 shows the schematic layout of FCSG connection to the grid using a full scale converter.

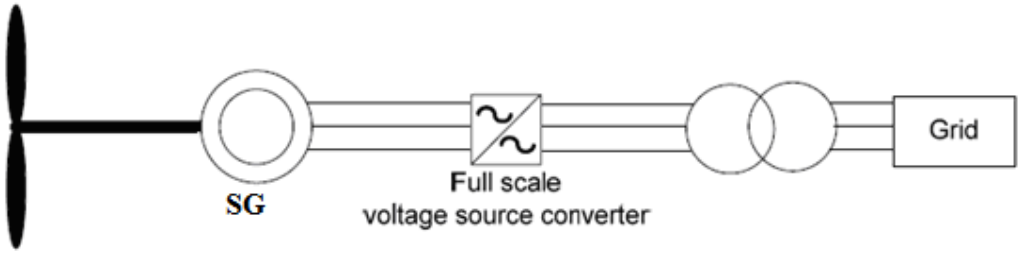

Figure 4- 4: A fully controlled synchronous generator connected to the grid with a full scale back to back voltage source converter in the stator side. (Source [12])

4.3 Implementation of wind turbines in RTDS

Generally it could be possible to implement either type of wind turbine models in RTDS but in RSCAD version of 1.204 there is no any dedicated wind turbine model.

For the implementation of SCIG it is possible to use the induction motor model in RSCAD with a positive mechanical torque input as shown in Figure 4- 5. This mechanical input torque is supplied by the wind turbine. For small scale wind farm connection the reactive power demanded by SCIG may not be too large. But for large wind farm production it is not easy to compensate for the consumed reactive power. For a connection of large wind farm at high voltage level with a real power in the GW range, the reactive power consumption could be too large. So, it is a must to compensate this huge reactive power demand by SCIG using a capacitor or other VAr compensation technique otherwise it may lead to voltage instability.

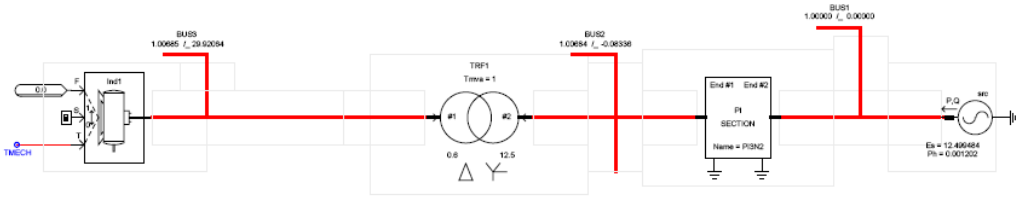

Figure 4- 5: grid connected induction generator in RSCAD. Positive mechanical torque input to the induction generator is derived from the wind turbine model as shown in Figure 4-1.

In the RTDS it is possible to implement the DFIG using the existing wound rotor induction generator and a back-to-back voltage source converter (VSC) at the rotor side as shown in Figure 4- 6. The wound rotor induction generator and the corresponding VSC are available in RSCAD library under small-time step model group. These small-time step models require a processor called GPC card. GPC card has a capability to perform all the computations of these models at time step that is much smaller compared to other power system component models. The maximum possible time step required to solve the model of DGIF and VSC is around 2.5 μs.

In the RTDS hardware set in HCPS group of Delft University of Technology the GPC cards are not available. As a result it is not possible to use the existing model of DFIG in RSCAD. Another alternative method to model DFIG is to use the control block components in RSCAD [13]. A controlled current source is used to inject the current coming from DFIG model which is developed using control block components. While using this model it is not possible to connect a power more than 35 MW otherwise the controlled current source component give numerical instability error. Even above 20 MW of power the injected current has some ripples. Hence, this model is not good enough to connect large wind farms of GW power.

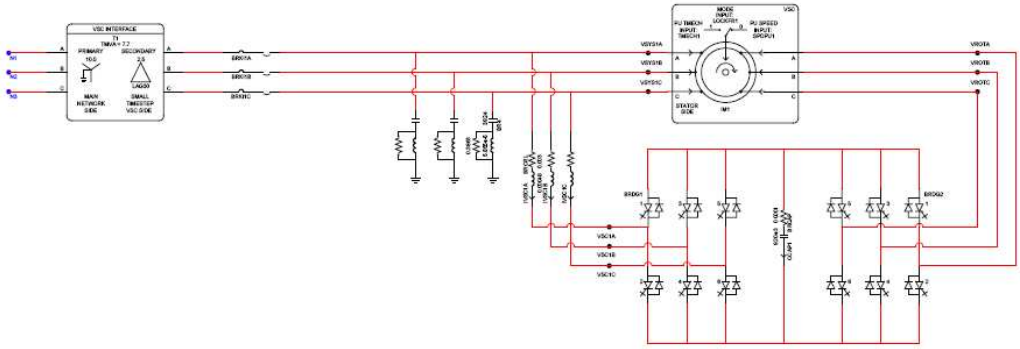

Figure 4- 6: the DFIG model developed in RSCAD. The voltage source converter is connected between the rotor and the stator side. The mechanical input torque to the generator is derived from the wind turbine model as shown in Figure 4-1.

According to [14] and [15] it is possible to model a FCSG in RTDS with the appropriate control system for the voltage source converter. Figure 4- 7 shows how a FCSG model can be implemented in RSCAD Draft module. It could be possible to use this model to study the nature of a give grid with installed wind power.

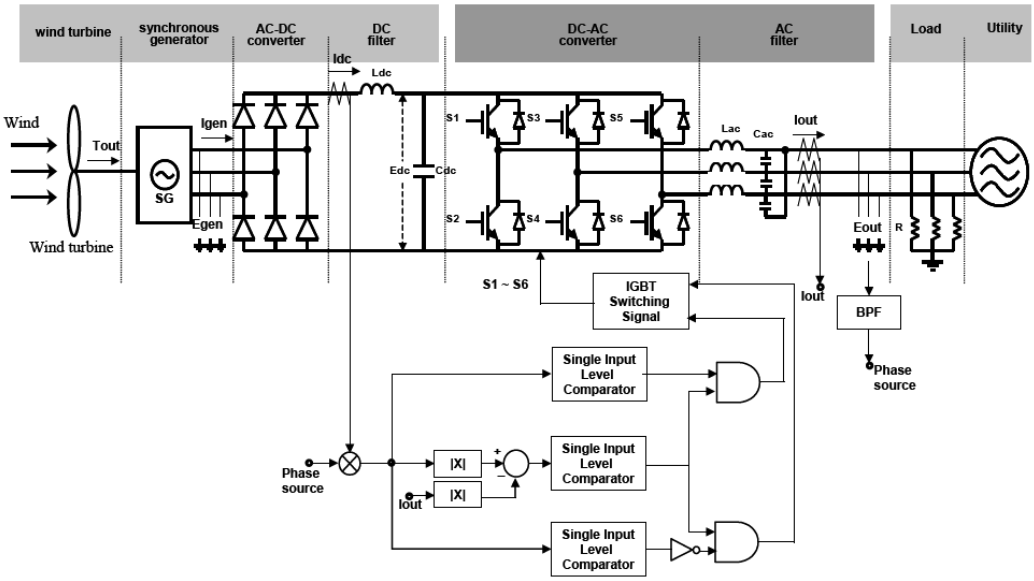

Figure 4- 7: synchronous generator connected to grid with a full scale voltage source converter. (Source [14])

Generally the off-shore wind farm is connected to the on-shore grid by using HVDC system. The HVDC system electrically decouples the wind farm system from the grid. Hence, the fault response of the wind farm is governed by the HVDC connection technology rather than the wind turbine technology used. The response of the HVDC system to the voltage dip caused by a fault is managed by limiting the current output of the converter [11].

As mention by [16] distributed generation source can be connected to the grid indirectly through a power electronic converter. These converter connected large wind power sources can be modelled either using a voltage source converter or using constant PQ-source model.

Based on [16] for power system dynamic study of large system, constant PQ- source model can be used. In this model the current injected to the grid by the grid side converter is the quantity of main interest. This current is derived from the active and reactive power supplied the grid side converter. The active power is coming from the wind. The equation for current injection is:

$$I_g = \frac{\eta P_w}{\sqrt{3} V_l \cos\theta} \tag{3.8}$$

Where, η= efficiency of the generator

cosθ= pf; power factor of at the coupling point

V_l = line voltage

P_w =wind power

Large wind farms connected to a grid via a full converter can be disconnected from the grid when the connection point voltage level drops below a predefined minimum value. It is possible to use two minimum voltage level algorithms [16] to control the current injected to the grid. The voltage ride through algorithm is defined as shown below:

Current calculation algorithm

Required: P_w (P_{nom}); cos θ; V_{min1}; V_{min2}; I_{max} (V_{l_rated})

if $V_l \geq V_{min1}$ **then**

$$I_g = \frac{\eta P_w}{\sqrt{3} V_l \cos\theta}$$

else if $V_{min1} \geq V_l \geq V_{min2}$ **then**

$I_g = I_{max}$ where $I_{\max} = \frac{\eta P_w}{\sqrt{3} V_{l\_rated} \cos\theta}$

else { $V_l < V_{min2}$ }

$I_g = 0$

4.4 Simulation results of Noord-Holland grid with large wind power input

After connecting 1.2 GW wind power to the existing Noord-Holland grid different simulation tests are conducted. The value of the voltage at all substations shows an average rise of 3%. With these initial voltages the following four tests are done to see the response of the expanded grid.

- A 3-phase to ground fault at Westwoud 150 kV substation.
- Loss of VN25 generator
- Rise in active power demand at Westwoud
- Reactive power demand reduction at Westwoud

Then the response of the voltage at Westwoud, Velsen, Diemen 380 kV and Hoogte Kadijk substations will be discussed. For all tests in this section the generators are equipped with the corresponding control systems; both excitation and governor.

Compared to the existing grid, after connecting 1.2 GW wind power the voltage level at substation raised. Figure 4- 8 below shows this comparison.

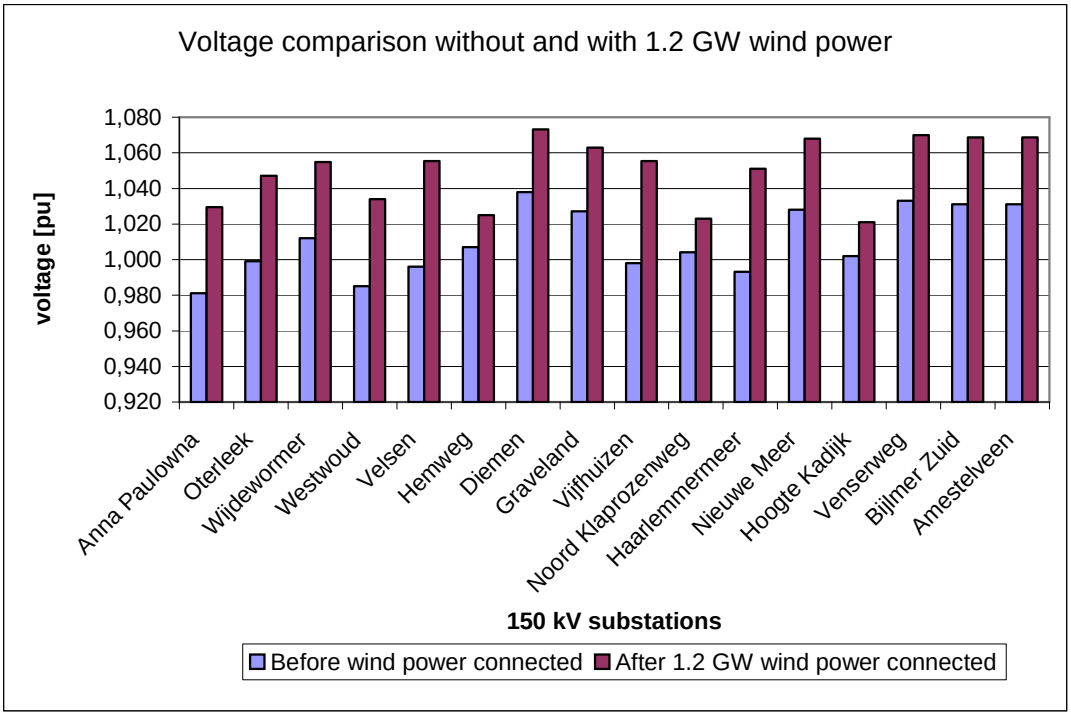

Figure 4- 8: Voltage value comparison before and after 1.2 GW wind power connection.

Dynamic test one: 3-phase to ground fault at Westwoud 150 kV

A 3-phase to ground fault is applied at Westwoud 150 kV substation with a fault duration of 100 ms. During this fault the voltage at Velsen drops below 0.8 pu hence the current coming from the constant PQ source model is limited to its rated value. However, it is still supplying around 80% of the rated power because the voltage drops is around 0.8 pu at Velsen.

Figure 4- 9 shows the voltage response for the 3-phase to ground fault at Westwoud 150 kV substation. After clearing the fault, the voltage response of the 150 kV substations clearly shows small oscillations. Compared to the 150 kV substations Diemen 380 kV substation shows no oscillation. Diemen 380 kV substation is the connection point to the external TenneT grid that is electrically very strong for such disturbances.

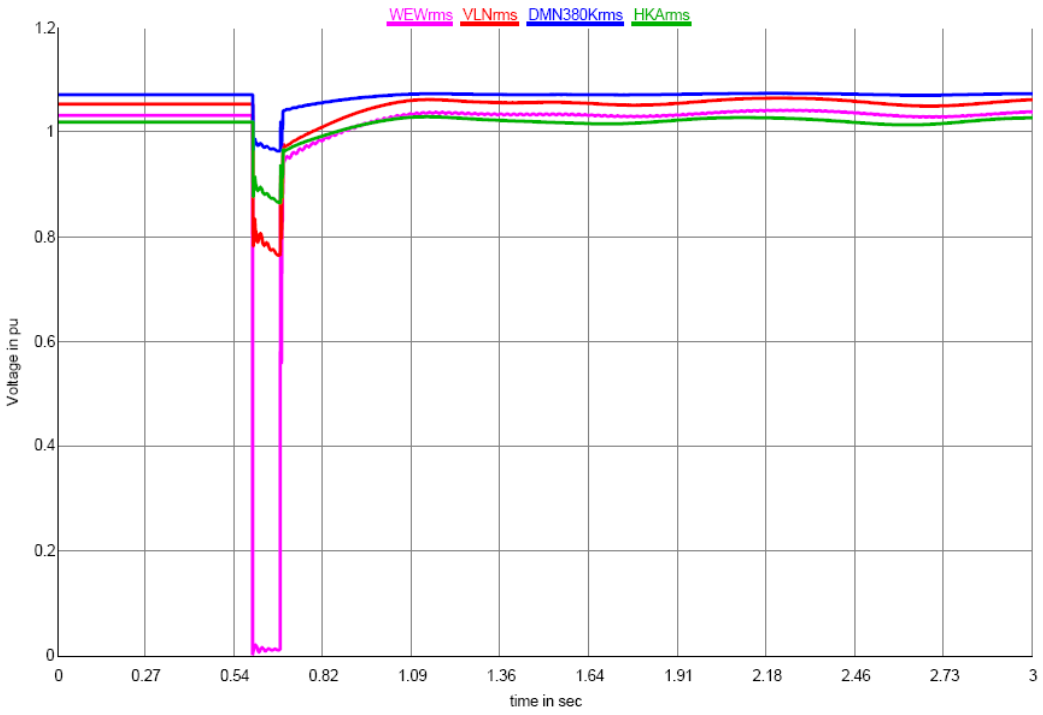

Figure 4- 9: Voltage response at Westwoud (WEWrms),Velsen (VLNrms), Diemen 380kV (DMN380Krms) and Hoogte Kadijk (HKArms) substations during a 3-pahse to ground fault at Westwoud 150 kV substation.

Figure 4-10 shows the voltage response at Westwoud, Velsen, Hoogte Kadijk and Diemen 380 kV substations during a 3-phase to ground fault at Westwoud before 1.2 GW wind power is connected at Velsen. From Figure 4- 9 and Figure 4- 10 it is possible to do comparison between the existing grid and the expanded grid with 1.2 GW wind power input. The comparison is based on the 3-phase to ground fault response at Westwoud 150 kV substation.

For the existing grid, i.e. without 1.2 GW wind power, the response of the voltage at the shown substations hardly shows any oscillations. Whereas after connecting 1.2 GW wind power the response of the voltage gives small oscillation but the oscillations are within narrow range. Compared to the response of the existing grid without wind power, it seems the connection of large wind power could lead to unstable condition.

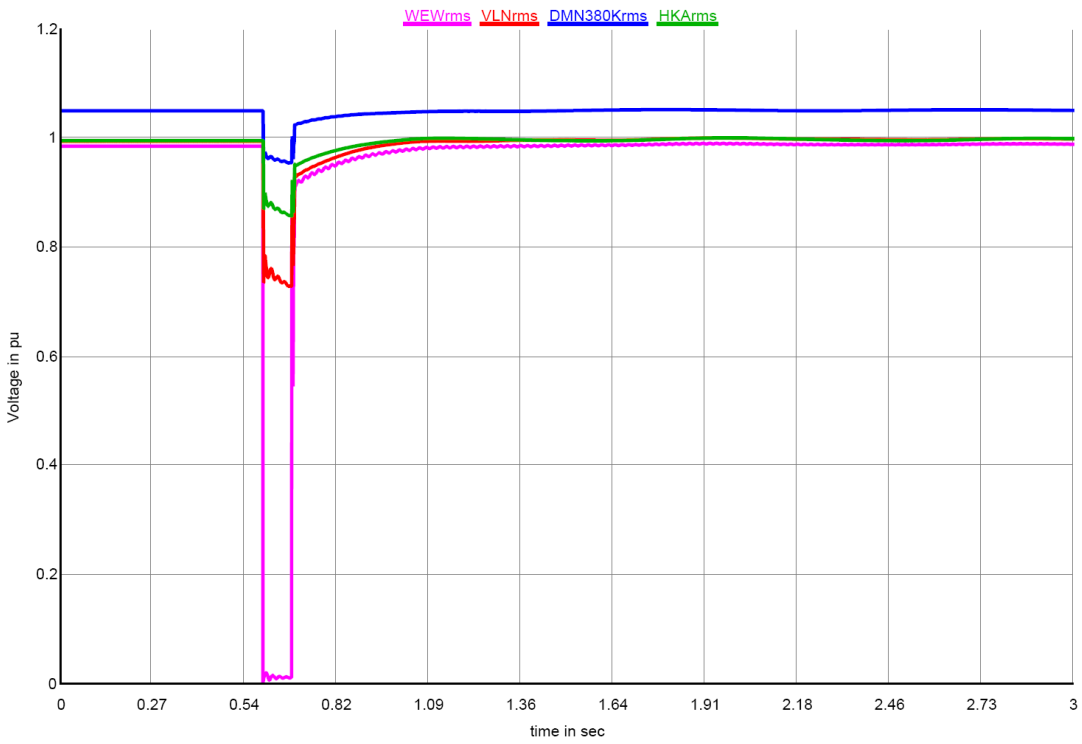

Figure 4- 10: Voltage response at Westwoud (WEWrms),Velsen (VLNrms), Diemen 380kV (DMN380Krms) and Hoogte Kadijk (HKArms) substations during a 3-pahse to ground fault at Westwoud 150 kV substation before connecting 1.2 GW wind power at Velsen 150 kV substation.

Dynamic test two: Reduction of active power generation at VN25 generator

The active power generated by VN25 generator at Velsen 150 kV substation is reduced from 360 MW to 45 MW by changing the setting point of the rated power from 0.86 pu to 0.125 pu. When the active power generated by VN25 generator decreased 315 MW, the grid gets the required amount of active power from the infinite voltage source. Figure 4- 11 shows the voltage responses at Westwoud, Velsen, Diemen 380 kV and Hoogte Kadijk substations when the active power generated by VN25 generator is decreased from 360 MW to 45 MW.

Due to the time settings of governor control, the generator takes few seconds to reach the stable operating point. During this time one can see the generator rotor oscillation on the voltage response of the near by substations. Once the system reaches the stable operating point the voltage damps and returns to its original value.

The voltage response from this test shows that the loss of a generator could not lead to major voltage instability as long as there is a strong connection (this case the infinite voltage source).

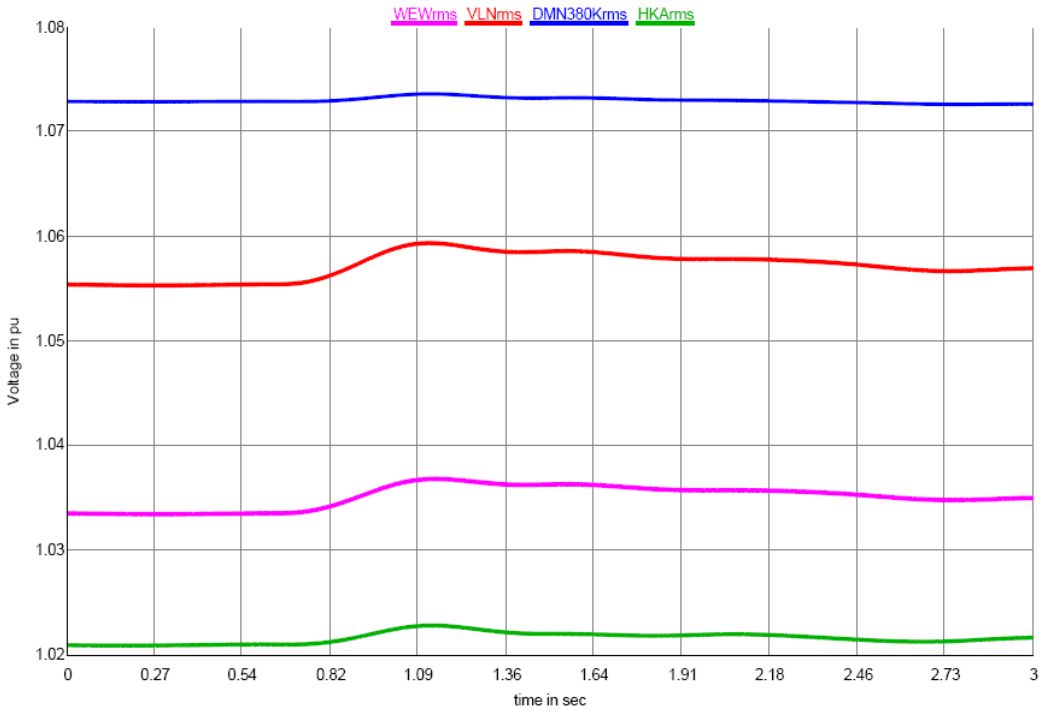

Figure 4- 11: Voltage response at Westwoud (WEWrms),Velsen (VLNrms), Diemen 380kV (DMN380Krms) and Hoogte Kadijk (HKArms) substations when VN25 generator reduces the active power generation.

Dynamic test three: rise in active power demand at Westwoud to 400 MW

For this test case it is assumed that the active load at Westwoud 150 kV substation rise from 163 MW to 400 MW without changing the reactive power demand. As shown in Figure 4- 12 the rise in the active load demand causes a voltage drop at all substations but at Westwoud the drop is large (around 3%).

Again in this case when the load raised to 400 MW the new 233 MW power demand is supplied by the infinite voltage source at Diemen 380 kV substation. During this power unbalance the central generators couldn't supply this power gap because they are PV generator types. Hence they keep supplying their rated power output only.

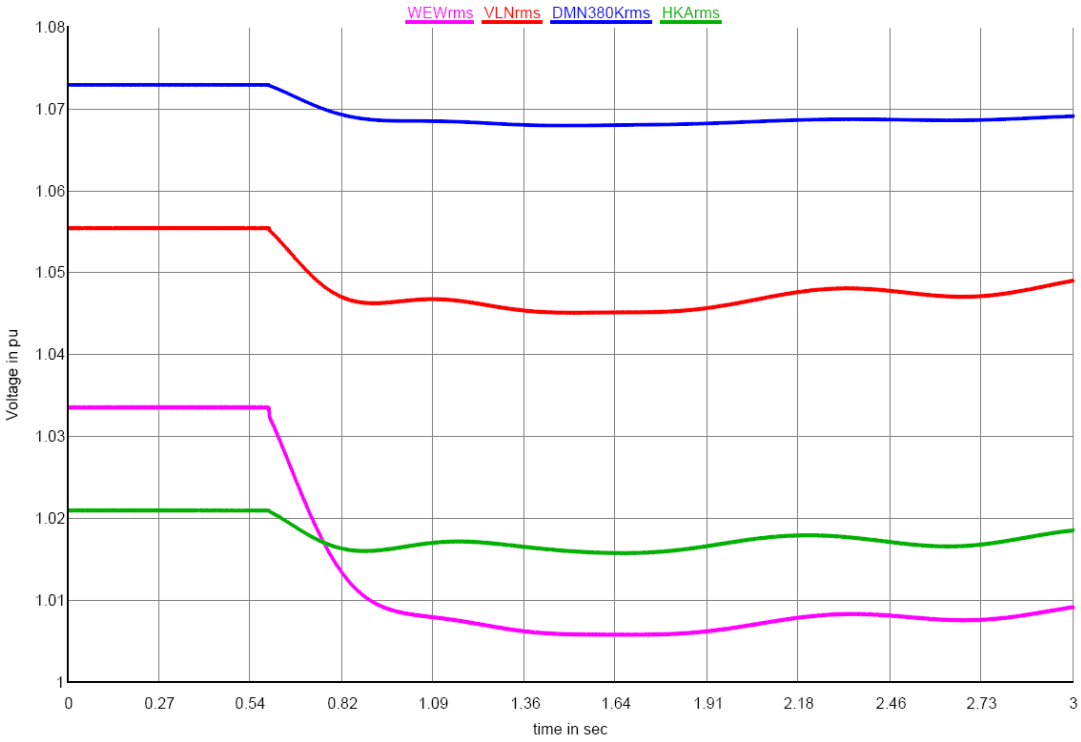

Figure 4- 12: Voltage response at Westwoud (WEWrms),Velsen (VLNrms), Diemen 380kV (DMN380Krms) and Hoogte Kadijk (HKArms) substations when the active power demand increased to 400MW at Westwood.

Dynamic test four: reduction of 48 MVAr reactive power demand at Westwoud

In this test the active power load is set to its original value and the reactive power demand of 48 MVAr is reduced to 0 MVAr. The reduction of this reactive load could be equivalent to the injection of that much reactive power locally at Westwoud 150 kV substation. The reduction of the reactive power demand resulted in the voltage rise at all substations as shown in Figure 4-13. Again the voltage rise at Westwoud 150 kV substation is very significant compared to other substations.

Generally if there is large amount of reactive power injection locally, the voltage level could rise by considerable amount.

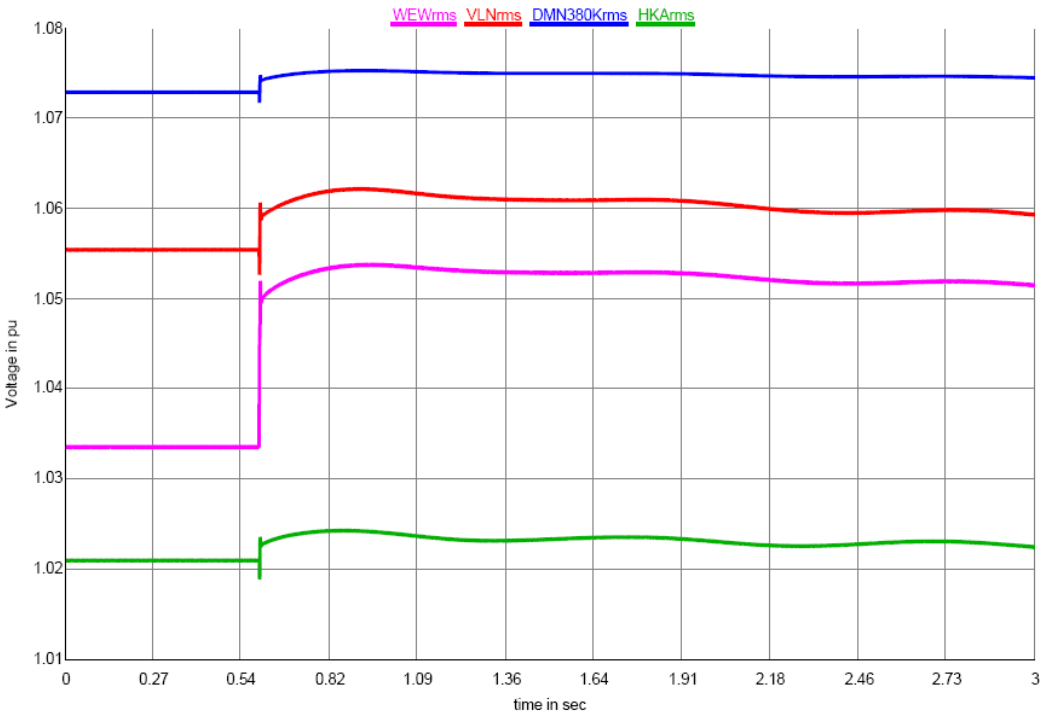

Figure 4- 13: Voltage response at Westwoud (WEWrms),Velsen (VLNrms), Diemen 380kV (DMN380Krms) and Hoogte Kadijk (HKArms) substations when a reactive power demands at Westwood decreased by 48 MVAr.

To summarise section 4.4, the following are the main points:

- The voltage response gives small oscillations after clearing a short-circuit fault.
- Reduction of active power generation shows immediate voltage rise but finally the voltage returns to its original value.
- The rise in active power demand decreases the voltage level at the substations. If there is a rise in active power demand in parallel to the wind power installation, the voltage levels at the substations could remain constant.
- The reduction of reactive power demand elevates the voltage level at the substations. Hence if there is a voltage drop problem the possible solution is to supply some amount of reactive power locally.

Chapter 5

Conclusions and Recommendations

5.1 Conclusions

The object of this thesis was to implement the existing grid of Noord-Holland with the future scenario extensions in RTDS, but due to some limitations it was not possible to implement the grid in real time simulation mode. The limitation is that some of the travelling wave transmission lines which are used as interconnecting lines between racks do not have the required travel time for real time simulation. The non-real time simulation mode is used to adjust the integration time step used in order to have the required travel time.

The grid is implemented and the validation is done based on non-real time simulation mode. Once the grid has validated the LC parameters of the travelling wave transmission lines can be modified to do a real time simulation.

The model in the RTDS is validated based on the non-real time simulation results. Steady state (load flow) value comparison is done with the VISION model. The magnitude and phase angle of the voltage for most substations are within 1% and 10% respectively. The line currents of most transmission lines are also within 10% error range. From the dynamic behaviour validation, the comparison with DIgSILENT model gives almost the same result; the general response behaviour of both models is comparable.

Due to the lack of GPC cards in RTDS hardware it was not possible to implement the existing DFIG model of wind turbine in RSCAD. Hence, the large wind power plant is connected to the grid with a simplified constant PQ source model. The connection of the wind power plan to the existing grid leads to voltage level rise at all substations. But if there is also a parallel load rise equivalent to the installed wind power, this voltage rise will not happen. Based on the short-circuit response, the dynamic behaviour of the grid with 1.2 GW installed wind power gives small oscillations hence it is relatively less stable than the existing grid.

5.2 Recommendations

Based on the following recommended ideas the RTDS model of Noord-Holland grid can be improved in future works.

1. Possible grid modifications

   - Once the RTDS model of Noord-Holland grid is validated based on the non-real time model, it is possible to use the modified model for real time simulation.
   - To use the RTDS model for real-time simulation, the line LC parameters must be changed to a possible minimum value of Table 3-2 to give the required travel time.
   - The transformers can be extended with corresponding load tap changers (LTC) but this option needs extra processors and increases the computation time required.

2. Expansion of the grid model with wind power plant

   On the RTDS model of Noord-Holland grid the wind power plant is implemented by simplified constant PQ source model. However, in the future work the exact model of the wind power plant could be implemented using either of the following options.

   - Remodel the existing DFIG model [13] from previous work in such a way that it can work at higher voltage levels.
   - Existing DFIG model in RSCAD with some changes in the existing hardware set. This option needs extra processor card that is not available this time.
   - By modelling the FCSG using the existing model in RSCAD. This option does not need new hardware cards like existing DFIG model. However, the corresponding converter control system must be modelled appropriately.

   Before connecting these wind farm models to the grid model, they must be verified first.

3. To implement other proposed extension scenarios to the RTDS model of Noord-Holland grid, first make sure the remaining numbers of processors are enough.

Appendix

A. Test data of Noord-Holland grid in RTDS

Table A- 1: Line currents in the RTDS model

Line name	Measured at	RTDS *I [A]*	VISION *I [A]*	I_% error
HW-NDK-WT	NDK	514	513	0.19%
HW-NDK-PS	NDK	516.4	515	0.27%
HK-NDK-WT	NDK	273.3	273	0.11%
HK-NDK-ZW	NDK	273.3	273	0.11%
HK-NDK-GS	NDK	273.3	273	0.11%
HW-VLN-WT	HW	1212	1220	-0.66%
VHZ-VLN-ZW	VHZ	340	332	2.41%
VHZ-VLN-WT	VHZ	334	326	2.45%
DMN-VW-WT	VW	780	771	1.17%
DMN-VW-ZW	VW	776	767	1.17%
VW-ZVD-ZW	ZVD	227.4	227	0.18%
HK-VW	HK	46	46	0.00%
VW-ZVD-GS	ZVD	227.4	227	0.18%
APL-OTL-ZW	APL	368	367	0.27%
OTL-WYW-WT	OTL	498.6	487	2.38%
OTL-WYW-GS	OTL	498.6	488	2.17%
DMN-WYW-GS	WYW	694.7	689	0.83%
DMN-WYW-WT	WYW	699.4	693	0.92%
BZ-VW-WT	VW	240	238	0.84%
BZ-VW-ZW	VW	240	238	0.84%
AMV-BN	BN	441	416	6.01%
AMV-BZ	BZ	90.3	96	-5.94%
HW-NDK-ZW	NDK	523.5	522	0.29%
DMN-GVL-ZW	GVL	418.7	419	-0.07%
DMN-GVL-WT	GVL	424.3	424	0.07%
DMN-WYW-ZW	WYW	699.8	694	0.84%
OTL-WEW-WT	WEW	336.2	336	0.06%
VHZ-VLN-GS	VHZ	290	285	1.75%
DMN-OSZ-ZW	DMN	474.9	474	0.19%
DMN-OSZ-WT	DMN	474.9	474	0.19%
AMV-DMN-ZW	AMV	506	508	-0.39%
NDK-NDP-E	NDK	245.3	243	0.95%
NDK-NDP-G	NDK	245.3	247	-0.69%
NDK-NDP-F	NDK	245.3	245	0.12%
BN-DMN	BN	548	539	1.67%
OTL-WYW-ZW	OTL	498.6	488	2.17%
NMR-VHZ	VHZ	428	384	11.46%
NMR-VW	NMR	475	458	3.71%

HMM-VHZ-WT	VHZ	268.5	266	0.94%
HMM-VHZ-ZW	VHZ	267.4	265	0.91%
BVW-OSZ-ZW	BVW	416.2	425	-2.07%
HW-OSZ-T401	OSZ T401	474.7	476	-0.27%
HW-OSZ-T402	OSZ T402	474.7	476	-0.27%
HW-OSZ-T403	OSZ T403	474.7	476	-0.27%
AMV-NMR	NMR	298.2	284	5.00%
APL-OTL-WT	APL	368.3	367	0.35%
OTL-WEW-ZW	WEW	336.2	336	0.06%
OTL-VLN-WT	OTL	385.1	382	0.81%
OTL-VLN-ZW	OTL	385.1	381	1.08%
404	DMN Tr404	466.7	465	0.37%
402	DMN Tr402	466.7	471	-0.91%
401	DMN Tr401	471.9	470	0.40%
403	DMN Tr403	460.2	460	0.04%
OSZ T401	OSZ Tr401	182.4	182	0.22%
OSZ T402	OSZ Tr402	182.4	182	0.22%
OSZ T403	OSZ Tr403	182.4	182	0.22%

B. Governor and Excitation System Data

Excitation and Governor Control System Parameters

Table B- 1: Excitation and Governor Control types [10]

Generator name	Excitation control type	Governor control type
HW-E8	EXST1 (set 3)	TGVO1
VN25	IEEEX2 (set 2)	TGVO1
IJM01	IEEEX2 (set 3)	TGVO1
DM33	SEXS (set 0)	TGVO1
AVI-1	SEXS (set 0)	TGVO1
AVI-3	SEXS (set 0)	TGVO1
AVI-2	SEXS (set 0)	TGVO1
Opwek-PU-1	SEXS (set 0)	TGVO1
HVCA	SEXS (set 0)	TGVO1

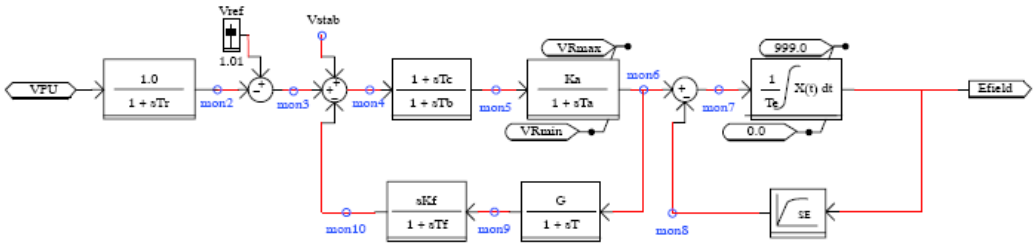

Figure B- 1: IEEEX2 Excitation control block diagram (source [6])

Table B- 2: IEEEX2 Excitation Parameters [10]

parameter	set 2	set3
Tr	0.01	0.01
Ka	1108	500
Ta	0.01	0.001
Tb	0.001	1
Tc	0	0
Te	0.5	0.3
Kf	0.022	0.022
Tf1	0.5	0.5
Tf2	1.2	0.2
Ke	1.2	0
E1	4	3.375
Se1	0.3	1.05
E2	2	4.5
Se2	1.5	1.5
Vrmin	-8	-8
Vrmax	9.8	9.8

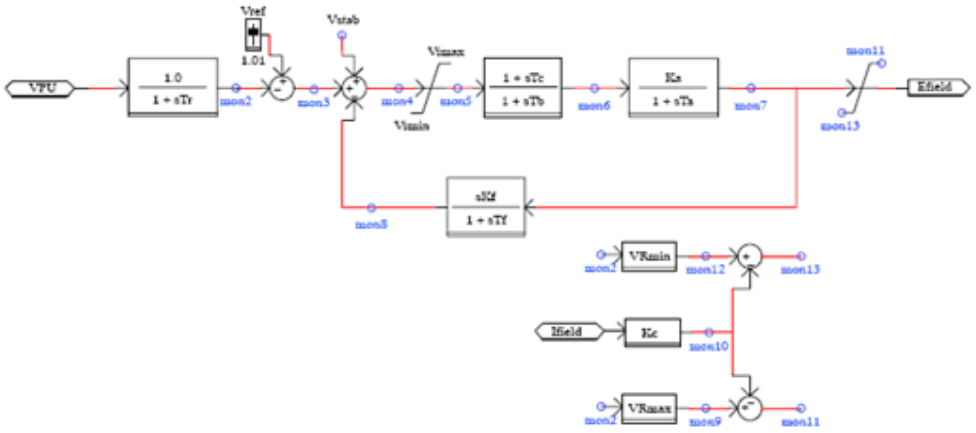

Figure B- 2: EXST1 excitation control block diagram (source [6])

Table B- 3: EXST1 Excitation parameters [10]

parameter	value
Tr	0
Tb	1
Tc	1
Ka	1000
Ta	0.01
Kc	0
Kf	0.015
Tf	2
Vimin	-3
Vrmin	-7
Vimax	10
Vrmax	4.9

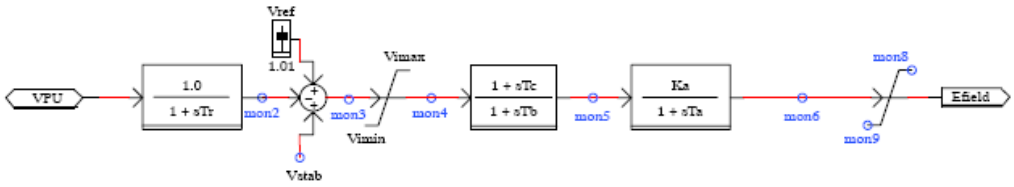

Figure B- 3: SEXS Excitation control block diagram (source [6])

Table B- 4: SEXS Excitation parameters [10]

parameter	value
Tb	0.9
Ta	10
K	35
Te	0.05
Emin	0
Emax	6

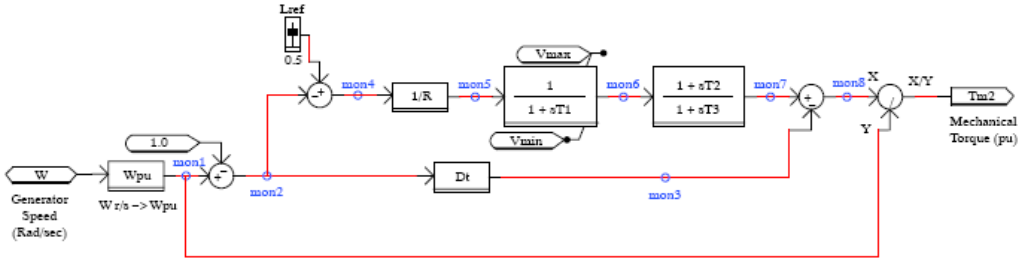

Figure B- 4: TGOV1 Governor Control block diagram (source [6])

Table B- 5: TGOV1 governor control Parameters [10]

parameter	value
T3	6
T2	2
At	1
Dt	0
Pturb	0
R	0.1
T1	0.5
Vmin	0.125
Vmax	2

C. System data of Noord-Holland grid in RTDS (confidential part)

References

[1] PSS/ETM 25, Program Application Guide, December 1997.

[2] P. Kundur, *Power system stability and control*, McGraw Hill: New York, 1994.

[3] DIgSILENT Manuals, DIgSILENT PowerFactory, Version 13, 2003.

[4] MATLAB, The Mathworks, Inc., Natick, MA, USA.

[5] Power System Analysis Toolbox, Documentation for PSAT, Version 1.3.4, July 2005.

[6] RTDS User Manual, Version 1.204, March 2007.

[7] *A Fully Digital Power System Simulator Operating in Real Time*, CCECE 1996, RTDS Technologies Inc., Winnipeg, Canada.

[8] KK Kaberere, KA Folly, M Ntombela, AI Petroianu, *Comparative Analysis and Numerical Validation of Industrial-grade Power System Simulation Tools*, Proceedings of the 15th PSCC, August 2005.

[9] Ministerie van Economische Zaken, *Connect 6000 MW: final report*, July 2004, Den Haag.

[10] J. A. Bos, *Connection of large-scale wind power generation to the Dutch electrical power system and its impact on dynamic behaviour*, Mater thesis, Delft University of Technology, August 2008.

[11] J.G. Slootweg, *Wind power modeling and impact on power system dynamics*, PhD-Thesis, Delft University of Technology, December 2003.

[12] Y. Zhou, P. Bauer, B. Ferreira, J. T. G. Pierik, *Wind park and grid integration issues*, IEEE, Young Researcher Symp 2006.

[13] I. J. Van Vliet, *Dynamic modeling of a wind turbine generator for the RTDS*, Master thesis, Delft University of Technology, 2005.

[14] J.-H. Kim, M. Park, I.-K. Yu, *Real time digital simulation of the wind power system using RTDS*. URL: http://www.eecu.net/~yuik/paper/paper12/paper1-31/1.pdf (last accessed date June 23,2009)

[15] S.-K. Kim, E.-S. Kim, I.-Y. Yoon and H.-Y. Kim, *PSCAD/EMTDC based dynamic modeling and analysis of a variable speed wind turbine*, Power Engineering Society General Meeting, 2004. IEEE

[16] M. Reza, *Stability analysis of transmission system with high penetration of distributed generation*, PhD-Thesis, Delft University of Technology, December 2006.